# แบบจำลองการเร่งที่คลื่นกระแทกในเวลาจำกัด

นายชาญเรืองฤทธิ์ จันทร์นอก



วิทยานิพนธ์นี้เป็นส่วนหนึ่งของการศึกษาตามหลักสูตรปริญญาวิทยาศาสตรดุษฎีบัณฑิต

สาขาวิชาฟิสิกส์ ภาควิชาฟิสิกส์

คณะวิทยาศาสตร์ จุฬาลงกรณ์มหาวิทยาลัย

ปีการศึกษา 2548

ISBN 974-53-2327-6

# MODELING OF FINITE TIME SHOCK ACCELERATION

Mr. Chanruangrit  Channok



A Dissertation Submitted in Partial Fulfillment of the Requirements

for the Degree of Doctor of Philosophy Program in Physics

Department of Physics

Faculty of Science

Chulalongkorn University

Academic year 2005

ISBN 974-53-2327-6

| | |
|---|---|
| Thesis Title | Modeling of Finite Time Shock Acceleration |
| By | Mr. Chanruangrit Channok |
| Filed of study | Physics |
| Thesis Advisor | Assistant Professor Udomsilp Pinsook, Ph.D. |
| Thesis Co-advisor | Associate Professor David Ruffolo, Ph.D. |

---

Accepted by the Faculty of Science, Chulalongkorn University in Partial Fulfillment of the Requirements for the Doctor's Degree

........................................................ Dean of the Faculty of Science

(Professor Piamsak Menasveta, Ph.D.)

THESIS COMMITTEE

........................................................ Chairman

(Assistant Professor Kajornyod Yoodee, Ph.D)

........................................................ Thesis Advisor

(Assistant Professor Udomsilp Pinsook, Ph.D)

........................................................ Thesis Co-advisor

(Associate Professor David Ruffolo, Ph.D.)

........................................................ Member

(Assistant Professor Patcha Chatraphorn, Ph.D)

........................................................ Member

(Burin Asavapibhop, Ph.D.)

........................................................ Member

(Pichet Kittara, Ph.D.)

ชาญเรืองฤทธิ์ จันทร์นอก : แบบจำลองการเร่งที่คลื่นกระแทกในเวลาจำกัด. (MODELING OF FINITE TIME SHOCK ACCELERATION) อ.ที่ปรึกษา : ผศ.ดร.อุดมศิลป์ ปิ่นสุข, อ.ที่ปรึกษาร่วม : รศ.ดร. เดวิด รูฟโฟโล 99 หน้า . ISBN 974-53-2327-6.

อนุภาคพลังงานสูงจากพายุสุริยะ ที่เป็นไอออนชนิดต่างๆ ถูกเร่งมาจากไอออนซุปปราเธอร์มอล (suprathermal) ที่มีอยู่แล้วโดยคลื่นกระแทกในตัวกลางระหว่างดาวเคราะห์ การสังเกตสเปกตรัมพบการโค้งลงที่ช่วงพลังงาน 0.1 – 10 MeV/นิวคลีออน ซึ่งได้มาจากช่วงเวลาจำกัดของการเร่งอนุภาค เราได้สร้างแบบจำลองของการเร่งอนุภาคในเวลาจำกัดเพื่ออธิบายเหตุการณ์การเร่งอนุภาคพลังงานสูงจากพายุสุริยะที่คลื่นกระแทกในตัวกลางระหว่างดาวเคราะห์บริเวณใกล้โลก โดยใช้ตัวแปรที่วัดได้จากคลื่นกระแทก แบบจำลองของการเร่งอนุภาคในเวลาจำกัดสามารถใช้ได้อย่างดีกับการวัดสเปกตรัมพลังงานของไอออน คาร์บอน ออกซิเจน และ เหล็ก โดยเครื่องวัด Ultra-Low-Energy Isotope Spectrometer (ULEIS) บนยานอวกาศ Advanced Composition Explorer ใน 3 เหตุการณ์ พบว่าระดับค่าที่ได้ของระยะอิสระเฉลี่ยในการเร่งในตัวกลางระหว่างดาวเคราะห์มีค่าปกติสำหรับเหตุการณ์ที่รุนแรงน้อย และมีค่าลดลงเป็น 0.003 AU สำหรับเหตุการณ์ที่รุนแรงมาก ซึ่งตรงกับความคิดจากผลของคลื่นที่ขยายเนื่องจากโปรตอน (proton-amplified wave) จากฟลักซ์อนุภาคที่สูงมากในเหตุการณ์ใหญ่



| | |
|---|---|
| ภาควิชา...ฟิสิกส์... | ลายมือชื่อนิสิต ............ |
| สาขาวิชา...ฟิสิกส์... | ลายมือชื่ออาจารย์ที่ปรึกษา............ |
| ปีการศึกษา...2548... | ลายมือชื่ออาจารย์ที่ปรึกษาร่วม......เดวิด รูฟโฟโล...... |

## 4573801623 : MAJOR PHYSICS

KEY WORD: SHOCK ACCELERATION / SUN / INTERPLANETARY MEDIUM / SOLAR EVENT

CHANRUANGRIT CHANNOK : MODELING OF FINITE TIME SHOCK ACCELERATION. THESIS ADVISOR : ASST. PROF. UDOMSILP PINSOOK, Ph.D., THESIS COADVISOR : ASSOC. PROF. DAVID RUFFOLO. Ph.D., 99 pp. ISBN 974-53-2327-6.

Energetic storm particles (ESP) of various ion species have been shown to arise from a suprathermal seed ions accelerated by traveling interplanetary shocks. The observed spectral rollovers at ~ 0.1 to 10 MeV/nucleon can be attributed to the finite time available for shock acceleration. We construct a finite time shock acceleration model for describing ESP events at interplanetary shocks near the Earth. Using the locally measured shock strength parameters as inputs, the finite-time shock acceleration model can successfully fit the energy spectra of carbon, oxygen, and iron ions measured by the Ultra-Low-Energy Isotope Spectrometer (ULEIS) on board the Advanced Composition Explorer during 3 ESP events. The inferred scattering mean free path in the acceleration region ranges from a typical interplanetary value for the weakest ESP event down to 0.003 AU for the strongest event. This is consistent with the idea that proton-amplified waves result from the very intense particle fluxes in major events.



Department ...Physics... Student's signature ..........

Field of study ...Physics... Advisor's signature ..........

Academic year ...2005... Co-advisor's signature..........

# Acknowledgements

The author wishes to express his sincere appreciation and gratitude to his advisors, Assoc. Prof. Dr. David Ruffolo, and Assist. Prof. Dr. Udomsilp Pinsook for great advice, guidance and encouragement given throughout the course of the investigation. He wishes to deeply thank his special advisors Prof. Dr. Glenn Mason and Dr. Mihir Desai from the University of Maryland at College Park, USA for observed data from the ULEIS instrument and supervising research work at the Space Physics Group, University of Maryland.

He would like to thank the members of his thesis committee, Assist. Prof. Dr. Kajornyod Yoodee, Assist. Prof. Dr. Patcha Chatraphorn, Dr. Burin Asavapibhop, and Dr. Pichet Kittara for reading and criticizing the manuscript.

He would like to thank present and former members of the space physics research group of Chulalongkorn University, especially for Dr. Tanin Nutaro, Dr. Alejandro Saiz, Dr. Piyanate Chuychai, Mr. Paisan Tooprakai, Mr. Kittipat Malakit, and Mr. Nimit Kimprapan.

He would like to thank his soul friends: Dr. Anucha Yangthaisong (A+), Dr. Anuson Niyompan (Pongo), Dr. Khomsorn Lomthaisong (Eat), Dr. Sriprajak Krongsuk (Jak), Dr. Paiboon Krutkaew, Teerachai Chamnanmor, Tanomsak Promprasit, Sarun Phibanchon, and Wuttisak Prachamon. Many thanks for his best love in the world to Assist. Prof. Dr. Nooduan Muangsan, and his pretty baby boy (Jett).

Finally, he would like to thank his family, his dad, his mom, and his sister.

This research was supported by a Chulalongkorn University research unit grant, the Thailand Research Fund, the Commission for Higher Education, and the Department of Physics, Chulalongkorn University.

# Contents

# List of Figures

# List of Tables

Page

# CHAPTER I
# INTRODUCTION

The Sun is the nearest star to the Earth, and has been studied for many thousands of years. When we observe the Sun with the eyes or in visible light, we may think that the Sun is quiet, but in reality the Sun has violent activity inside and outside (see Figure 1.1). The Sun has been the main power source to give light and heat to the Earth for billions of years. The Sun is the greatest natural energetic particle accelerator in our solar system, producing high energy particles up to 10 GeV (Lin 2003). The Earth is frequently hit by high energy particles from the Sun, and these particles have strong effects on Earth's atmosphere (see Figure 1.2). Effects on the Earth's atmosphere from high energetic particles generated during explosive solar activity can damage satellites and endanger working astronauts, and also passengers of high-altitude flights over polar regions (Lang 2000).

The research study of solar energetic particles (SEP) from the Sun is of great importance for modern space physics, especially research about the Sun and various effects on human activities near Earth.

In the past, there were many ideas about mechanisms of energetic particle acceleration at the Sun, a process that is not clearly understood. In 1942, from measurements in sea-level ion chambers on the Earth, the flux of SEPs was first

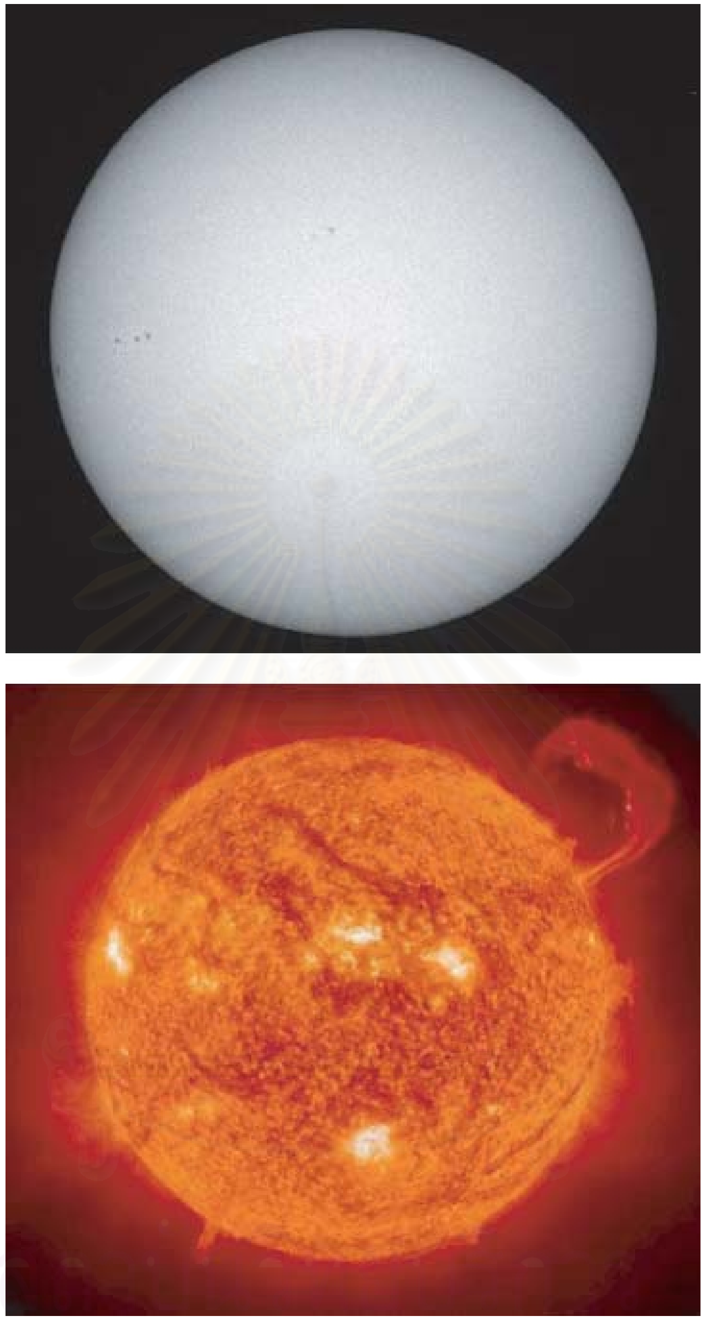

Figure 1.1: Images of the Sun, (top) observed in visible light by a ground-based telescope, (bottom) observed by the Extreme-Ultraviolet Imaging Telescope (in the He II 304Å line) on board the SOHO spacecraft. The bottom figure shows that the Sun has complicated structure on the surface, which can result in explosions and ejections of particles into space. [Picture credit: (top) Big Bear Solar Observatory, (bottom) Solar and Heliospheric Observatory]

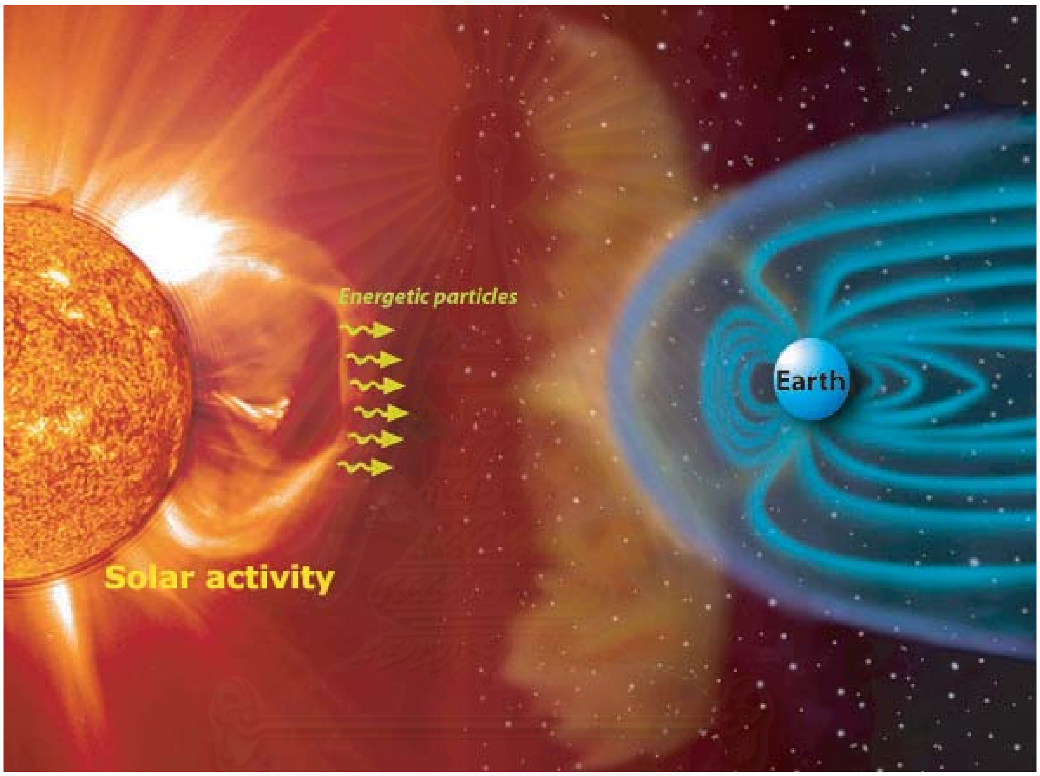


Figure 1.2: Illustration of energetic particles ejected from the Sun that may impact the Earth.

measured, with a sudden increase associated with a large solar event (Forbush 1946). After that SEPs have been observed in space by satellites launched since the 1950's. Nowadays with new instruments, we can study and observe many phenomena about the Sun and SEPs better than in the past, with data from many modern spacecraft (e.g. ACE, IMP, ISEE, SAMPEX, SOHO, WIND, Ulysses, Yohkoh, etc.) and satellites that were developed by scientists around the world. Recent SEP observations from modern spacecraft can give details about elemental composition of the Sun, ionic charge states, time profiles, energy spectra, particle abundances, etc. (Stone et al. 1998) in each SEP event.

From observations, solar eruptions at the surface of the Sun are the sources of SEPs that directly affect the Earth. Some SEP events are not strong, and some SEP events are very strong and large. The large SEP events produce enhanced particle fluxes in near-Earth space which typically persist for several days. Scientists classified the type of solar eruption (or solar flare) as "impulsive" and "gradual" by X-ray flare observation (Pallvicini et al. 1977; Miller 1998; Ruffolo 2002). Impulsive events are typical SEP events that involve stochastic acceleration at the flare site. Gradual events are very strong and large events that occur high in the corona of the Sun (Miller 1998) and are associated with coronal mass ejections (CME). The bulk of SEP are accelerated by CME-driven shocks (for more details see Chapter 2). When considering large events in which SEP are accelerated to high energy (above 10 MeV, Tylka et al. 1997) by interplanetary (IP) shock acceleration, the flux of SEP during strong events is high enough to affect Earth's magnetic field, Earth's atmosphere, and human activities on Earth. Effects from SEP events on the Earth include magnetic field variations that can cause problems for attitude control of spacecraft and compass usage. Ionospheric

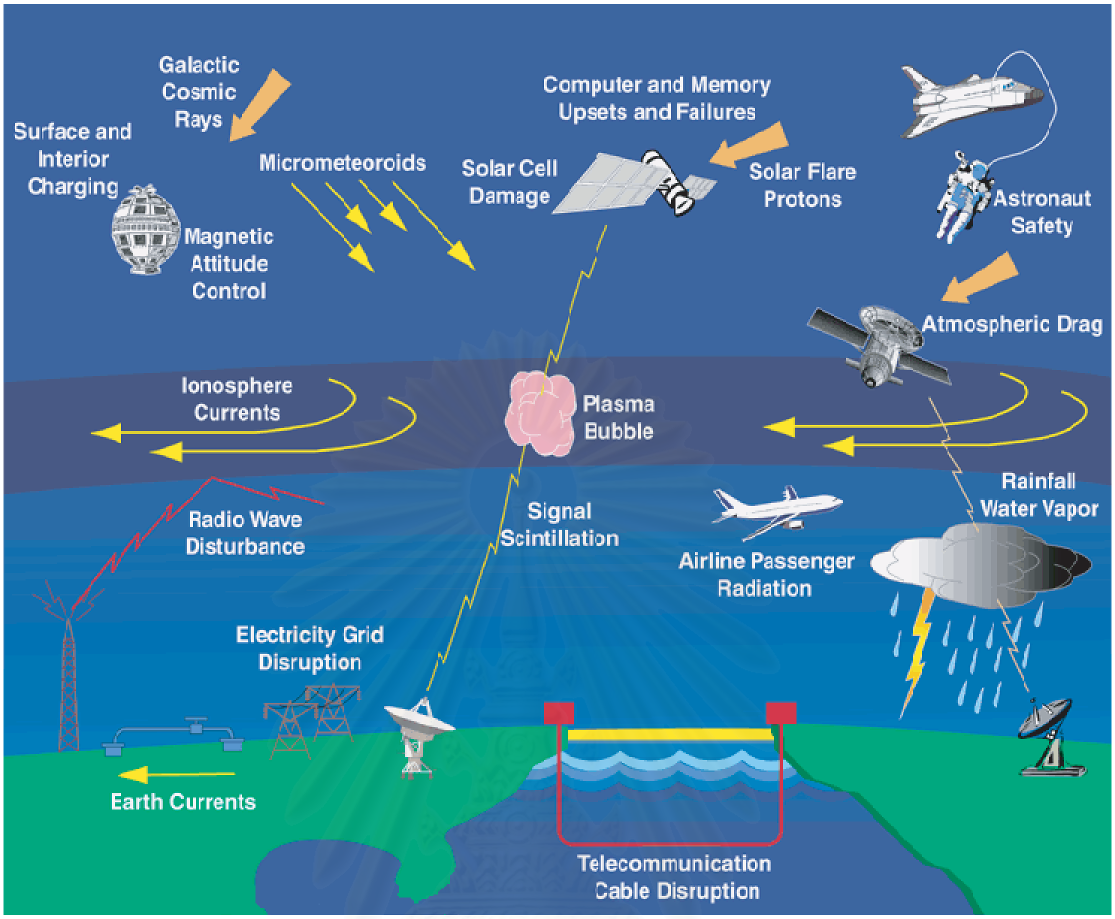


Figure 1.3: Effects of solar particle events on human activities near Earth, called "space weather effects." [Picture credit: L. Lanzerotti, Lucent Technologies]

variations can cause induction of electric currents in the Earth which disturb electric power distribution systems, long communication cables, telephone lines, radio and TV signal reflection, and communication satellite signals. SEP also pose a danger to astronauts in space and airplane passengers at high latitudes (see various effects on the Earth in Figure 1.3). These effects from solar strong events on human activities near Earth are called "space weather effects."

Specific examples of important SEP events affecting the Earth:

• On March 1989, an SEP event from a flare/CME explosion ejected a big plasmoid that reached the Earth after a couple of days. It compressed the Earth's magnetic field, which drove by induction an electric current systems and caused power outages in Canada. The SMM satellite was slowed down, its altitude falling by 1 km. Also a great aurora was produced which was seen as far South as Italy and Jamaica (Kirk, Melrose, and Priest 1994).

• On May 1998, during SEP events, high energy charged particles caused failure of electronic systems of expensive satellites, blanking out 80 percent of telephone-pager customers in the USA (Campbell 2001).

In this work we focus on important SEP events in which charged particles and ions from the Sun are accelerated to high energies by traveling IP shocks impact the Earth (referred to as "energetic storm particles", see details in Chapter 2). A powerful type of observation for understanding SEP events is the energy spectra from each SEP event. The energy spectra contain information about SEP production, sources of SEP events, and especially characteristics of particle acceleration. From observations of SEP events, it is found that energy spectra of solar energetic ions involve mechanisms of particle acceleration by IP shocks that produce spectral "cut-offs" at high energy (Ellison and Ramaty 1985; Tylka 2002; Desai et al. 2003, 2004). These spectra are not power laws like typical galactic cosmic rays (GCR) which come from outside the solar system. Observations of energy spectra of solar energetic ions from the ULEIS instrument on the ACE spacecraft near Earth found that the cut-off energy occurs at $\sim$ 0.1 to 10 MeV per nucleon (Desai et al. 2003, 2004). This observation is the motivation for our research work. We would like to explain characteristic energy spectra of IP shock accelerated particles by constructing a theory of finite time shock acceleration.

In the past, the idea for describing spectra of solar particle events in which SEP are accelerated by IP shocks in terms of a rollover energy was proposed by Forman (1981) and Ellison and Ramaty (1985). Energy spectra of SEP from IP shock events can be fitted with a famous formula by Ellison and Ramaty (1985), in which the energy spectrum has an exponential rollover term. The spectrum is assumed to roll over at a characteristic cut-off energy, $E_c$, as shown in equation (1.1):

$$N(E) \propto E^{-\gamma} \exp(-E/E_c), \tag{1.1}$$

where $N(E)$ is the energy distribution function, $E$ is the kinetic energy, and $\gamma$ is the shock spectral index.

Ellison and Ramaty (1985) suggested that various physical mechanisms could possibly lead to such a rollover, and each mechanism could yield a different value of $E_c$. This empirical formula is still used to fit spectra of impulsive and gradual solar particle events in many research works (e.g., Tylka et al. 2000, 2002; Tylka 2001; Desai et al. 2003, 2004; Klecker et al. 2003).

In this work we explore a specific mechanism for the rollover. We propose that the physical origin of the rollover is the finite time available for shock acceleration. The typical acceleration timescale corresponding to observed interplanetary scattering mean free paths is on the order of several days, so the process of shock acceleration at an IP shock near Earth should usually give only a mild increase in energy to an existing seed particle population (Ruffolo and Channok 2003). Indeed, a recent analysis of ACE/ULEIS observations argues for a seed population at substantially higher energies than the typical solar wind (Desai et al. 2003, 2004).

Our work derives a simple theory of finite-time shock acceleration and explores implications for the composition dependence of the spectrum. Note that finite-time shock acceleration should yield the standard power-law spectrum in the limit of a long duration time relative to the acceleration timescale. As a corollary of this idea, for an unusually strong shock (unusually short acceleration timescale) it is possible to obtain power-law spectra up to high energies (e.g., as observed by Reames et al. 1997). Then this is essentially infinite-time shock acceleration, in which other processes may limit the Fermi shock mechanism and lead to rollover energy spectra.

The main aim of this research work is to construct a model of finite time acceleration of SEP at IP shocks to describe characteristics of energetic storm particle (ESP) spectra.

The usefulness of our work is as follows:

- We use the finite time shock acceleration model to describe general characteristics of the ESP spectra for individual SEP events.
- We can quantitatively fit spectra from observed data from the ACE spacecraft in terms the finite time of IP shock passage near the Earth.

The other chapters in this thesis are organized as follows: The basic knowledge and theoretical background about SEP, ESP, and shock acceleration mechanisms are given in Chapter 2. The finite time shock acceleration model and mathematical formulation are described in Chapter 3. The results of numerical simulations from ESP events are presented in detail in Chapter 4. The discussion and conclusions of this work are presented in Chapter 5.

# CHAPTER II
# BACKGROUND KNOWLEDGE

Acceleration of energetic charged particles by magnetohydrodynamic shock waves is a universal mechanism in space astrophysics phenomena for explaining how charged particles reach very high energies in various astrophysical situations, such as supernova remnants (SNR) accelerating galactic cosmic rays (GCR) (Axford 1981a, 1981b; Lagage and Cesarky 1983b; Jokipii 1987; Gieseler, Jones and Kang 2000), active galactic nuclei (AGN) accelerating extra-galactic cosmic rays (EGCR) (Jones and Ellison 1991) beyond our solar system, and the acceleration of solar energetic particles (SEP) at the Sun and through IP space in the solar system (Reames 1999). Mason, Gloeckler, and Hovestadt (1984), Lee and Ryan (1986), Reames (1990) and Ruffolo (1997) have suggested that SEP associated with solar flare eruptions are accelerated by shock waves produced by flare explosions or coronal mass ejections (CMEs) at the Sun.

The study of acceleration of SEP is of great importance in space astrophysics since SEPs are primary cosmic rays, and characteristics of SEP (e.g., energy spectrum, time profile of intensity, directions of arrival of SEP, shock properties, ionic composition, etc.) are not very much disturbed during propagation through IP space (over only 1 AU) when compared with GCR or EGCR.

In this chapter we will provide background knowledge about the Sun, interplanetary magnetic field, solar energetic particles, energetic storm particles (ESP), observations of ESP, and concepts about astrophysical shock acceleration mechanisms for high energy particles in space physics.

## 2.1 The Sun and Interplanetary Magnetic Fields

The Sun is the nearest star to the Earth. The distance from the Earth to the Sun is about 1.5x$10^8$ km. (Astronomers define the distance from the Sun to the Earth a one Astronomical Unit, 1 AU). The Sun is a huge ball of hot dense plasma. The Sun is a perfectly ordinary star, and like the other stars it is large and massive. The Sun is the main source of space plasmas throughout the solar system.

The structure of the Sun can be divided into 4 zones (Foukal 1990; Cravens 1997; Lang 2001):

(1) **The core** is the center of the Sun which is high density plasma at a very high temperature (about 15 million K). One half of the mass of the Sun is contained in the core. The Sun's energy is generated in the core by the thermonuclear reactions.

(2) **The radiation zone** is the zone where energy is transported from the core by radiation.

(3) **The convection zone** is the zone where energy is transported by convection.

(4) **The atmosphere** is the region that can be directly observed from the Earth. Some amount of energy from the atmosphere region is converted to kinetic energy of particles, such as solar energetic particles and the solar wind. The

atmosphere can be divided into 3 regions: the photosphere, the chromosphere, and the corona.

The Sun can generate magnetic fields that emerge from sunspots on the solar photosphere. Sunspots have lateral dimensions of about 10,000 km (the largest sunspots can exceed 20,000 km, Foukal 1990) and they support magnetic fields with intensities of about 0.1 to several Tesla (Parks 1991). From many sunspots, the Sun has an average magnetic field intensity of about $10^{-4}$ Tesla (Parks 1991; Longair 1992).

The solar wind plasma from the solar corona flows into interplanetary space with a speed of about 250-800 km/s (Kallenrode 2001; Lang 2001). Since the conductivity of the solar wind plasma is high, the solar magnetic fields are frozen into it and carried out into interplanetary space. The solar wind plasma does not flow along magnetic field lines (Cravens 1997) but flows radially (or almost radially) outward from the Sun. The solar magnetic field lines widely expand in interplanetary space due to the effect of solar wind plasma flow. The convected solar magnetic field becomes the "interplanetary magnetic field" (IMF) (see Figure 2.1). The rotation of the Sun draws the configuration of the IMF into an Archimedean spiral (Parker 1958b) in the ecliptic plane. The fluctuation in the solar wind plasma flow causes the irregularity in the IMF. The IMF has a magnetic intensity of about $5 \times 10^{-9}$ Tesla on average near Earth, but is highly variable.

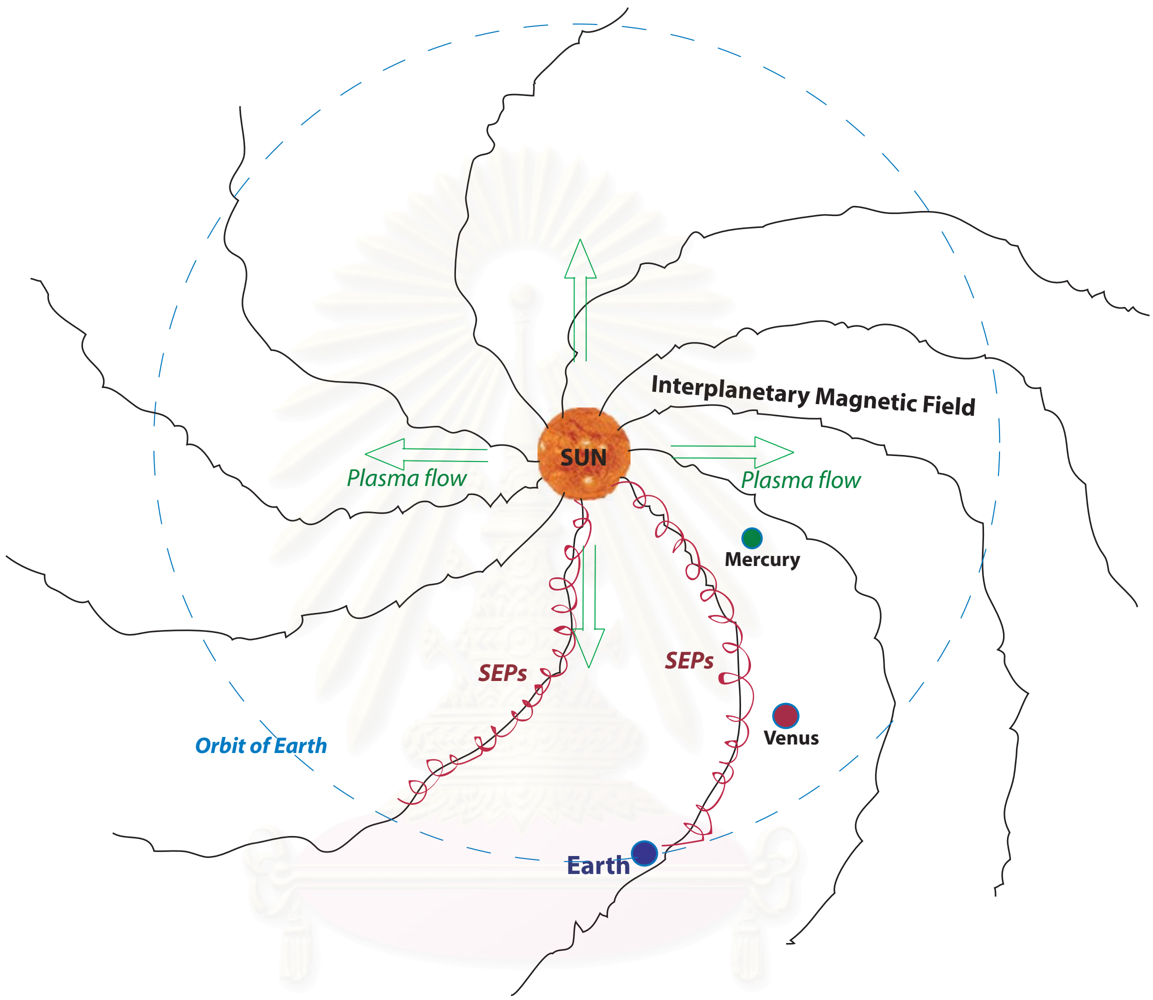


Figure 2.1: Structure of the interplanetary magnetic field from the Sun in the inner solar system to a distance 1 AU (size of the Sun and planets not to scale).

## 2.2 Solar Energetic Particles

Solar energetic particles (SEPs) are a type of cosmic rays, also called solar cosmic rays. SEP are high energy ions above 100 keV from the Sun that are accelerated in solar flare/CME eruptions. The energy of SEPs is much greater than the typical solar wind (e.g., solar wind protons at a speed of 500 km/s have a kinetic energy of about 1 keV in the spacecraft frame; Desai et al. 2003). SEPs are mainly protons, electrons, $\alpha$-particles, and heavy ions up to Fe.

The first discovery of SEP was in February 1942 by measurements in ion chambers on Earth. These measured a sudden increase in the particle flux which was associated with a solar flare (Forbush 1946). After that for many years, observations of SEP developed to use neutron monitors (e.g., Simpson 1948; Lockwood, Webber, and Hsieh 1974; Usoskin et al. 1997; Clem and Dorman 2000), reometers (Reames 1995), and modern instruments on spacecraft outside the Earth (e.g., Desai et al. 2003, 2004). Recent SEP observations from modern spacecraft instruments can give many details about SEP events such as the time profiles of intensity, energy spectrum, particle density, composition of elements, etc.

SEPs events can be divided into 2 classes: *impulsive* and *gradual* events (e.g., Cane et al. 1986; Reames 1999; Usoskin and Mursula 2001; Ruffolo 2002). Impulsive events are usually of relatively low intensity and short duration. "Impulsive" solar flares are typically defined as those with a short duration (less than 1 hour) of X-ray emission (Ruffolo 1997). Impulsive SEP events occur at flare sites near the surface of the Sun. Impulsive solar flares eject particles such as protons and electrons into IP space with energies up to millions of times greater than those in the normal solar wind. Typical maximum energies in these impul-

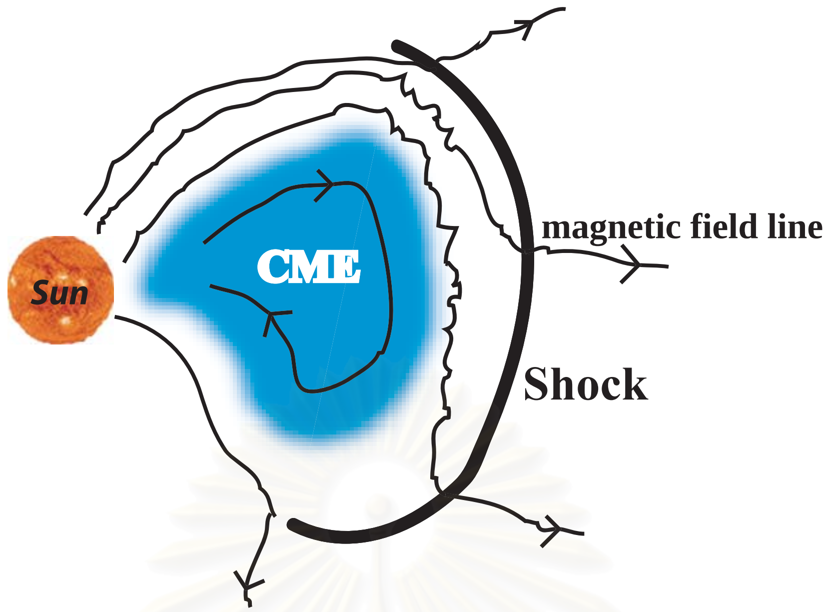


Figure 2.2: A large CME leads to a large magnetic cloud of plasma that drives a shock through interplanetary space. [Picture credit: Leerungnavarat (2004)]

sive events are less than 10 MeV/nucleon (Vainio and Khan 2004). The rate of impulsive events occurring at the Sun is about 1000 events per year (Tylka 2001).

For the large or "gradual" SEP events, SEP are accelerated at shock waves driven out from the Sun by fast coronal mass ejections (CMEs) producing high energy particles. (Reames 1999; Tylka 2001; Ruffolo 2002).

CMEs have speeds from about 100 km/s up to greater than 2000 km/s (Kallenrode 2001; Aschwanden 2004; Manchester et al. 2005). Fast CMEs have been measured up to speeds of 2505 km/s (on April 15, 2001; Gopalswamy et al. 2003). When considering that the solar wind has a typical speed of about 400-800 km/s, a fast CME is supersonic with respect to the solar wind. Thus, such a fast CME can drive a transient IP shock. A CME often leads to a very big hot plasma magnetic cloud (mass is about $10^{12} - 10^{13}$ kg, National Research Council 2004;

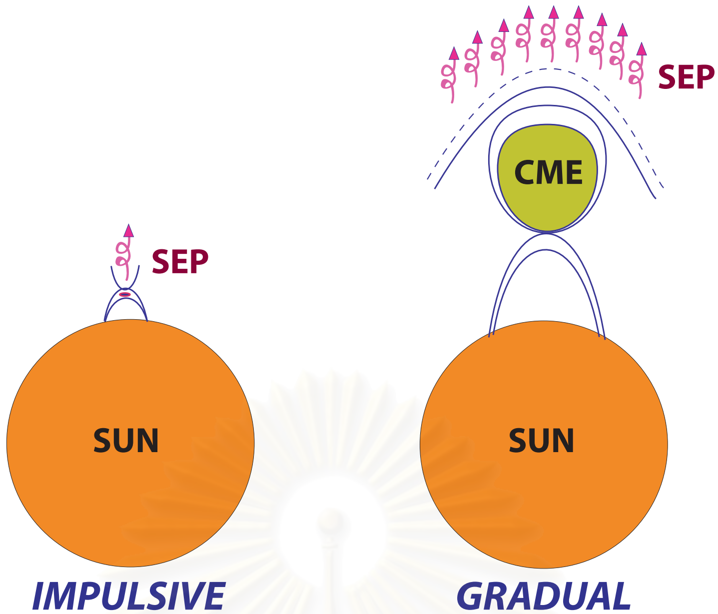


Figure 2.3: Illustration of impulsive and gradual events at the Sun. [Picture credit: Reames (1999) and Cliver (2000)]

Zhang and Low 2005; Manchester et al. 2005) moving with a very high speed into IP space, and to an IP shock located at the front edge of the plasma magnetic cloud (see Figure 2.2). Gradual events can have high-intensity peaks (more than $10^7$ proton/cm$^{-2}$) and long durations. The observed rate of large SEP events is about 6 events per year (Tylka 2001). Energy of SEP in large events are higher than impulsive events that are 100 keV to 30 GeV (Tylka 2001).

SEP observed in IP space exhibit different features, depending on whether the parent flare is impulsive or gradual (Cane, McGuire, and von Rosenvinge 1986; Kallenrode, Cliver, and Wibberenz 1992). Figure 2.3 shows characteristic differences of impulsive and gradual flares at the Sun. Table 2.1 lists different properties of impulsive and gradual flares.

The particles in most large events are accelerated over a large spatial

Table 2.1 Properties of SEP events following impulsive and gradual flares. Data from Cliver (2000), Kallenrode (2001), and Lang (2001).

| Event | impulsive flare | gradual flare |
|---|---|---|
| Particles | electron-rich | proton-rich |
| $^3He/^4He$ | $\sim 1$ | $\sim 0.0005$ (coronal) |
| H/He | $\sim 10$ (coronal) | $\sim 100$ |
| Fe/O | $\sim 1.23$ | $\sim 0.15$ (coronal) |
| Longitudinal cone | $\leq 30$ degrees | $\leq 180$ degrees |
| Duration of SEP event | $\sim 1$ hour | $\sim$ several days |
| Loop height | $\leq 10^4$ km | $\sim 5 \times 10^4$ km |
| Loop volume | $10^{26}$–$10^{27}$ cm$^3$ | $10^{28}$–$10^{29}$ cm$^3$ |
| Duration of X-ray emission | short (minutes, hard X-rays) | long (hours, soft X-rays) |
| Radio bursts | Types III and V | Types II and IV |
| Maximum energy | $\sim 10$ MeV | up to 50 GeV |
| Events per year | $\leq 1000$ | 6 |
| Coronagraph | Nothing detected | CME, 96% |

region by a shock wave at the head of a CME, not in a solar flare (Reames 1995). The CME-driven shock can accelerate SEP to high energy by a shock acceleration mechanism (Fermi 1954).

## 2.3 Energetic Storm Particles

Energetic storm particles (ESP) are energetic particles accelerated at IP traveling shocks (Lee 1983; Kallenrode 2001; Ho et al. 2003). Originally, ESPs were first observed on September, 1961 by Bryant et al. (1962). ESPs were found to be particle enhancements related to the passage of IP shocks. ESPs can be detected up to 20 MeV. Since IP shocks propagating to impact the Earth often cause *"Geomagnetic storms"* (magnetic storms on the Earth due to solar activity (Christian et al. 1997), see Figure 2.4); therefore, the particle enhancements have been called ESP events (Rao, McCracken and Bukata 1967). Van Allen and Ness (1967) proposed the Fermi shock acceleration of energetic particles between the propagating shock and upstream interplanetary magnetic field irregularities to explain the ESP enhancements.

We now understand that the same CME-driven shock accelerates particles in very different physical environments near the Sun and in interplanetary space. The SEP accelerated when the CME was near the Sun can remain present in IP space for several days and can greatly alter the time-intensity profiles of the ESP event (Scholer and Morfill 1975).

From past observations most ESP events exhibit a steepening of the spectrum at energies greater than $\sim 1$ MeV and an abrupt flux decrease some time after the passage of an IP shock wave (e.g., Bryant et al. 1962; Rao, McCracken and Bukata 1967). The improved instrumentation on the ISEE spacecraft enabled

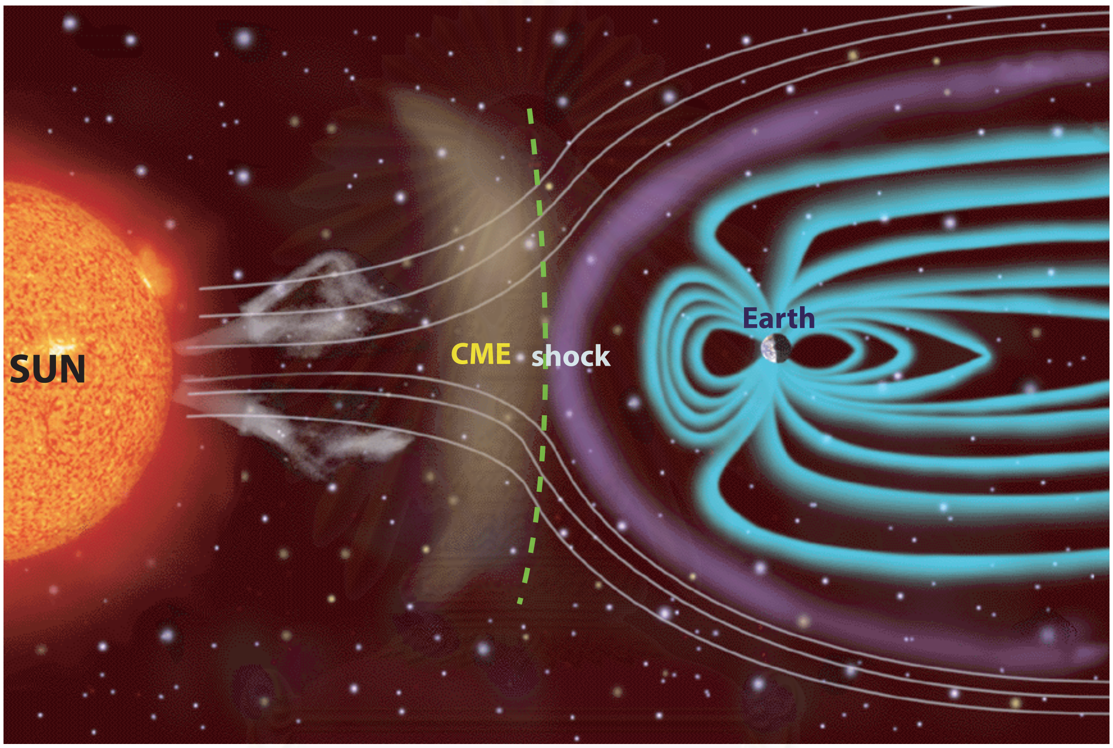


Figure 2.4: Illustration of ESP event in which a shock wave from a huge CME propagate to impact the Earth's magnetic field (not to scale). [Image credit: SOHO observatory (NASA/ESA)]

scientists to make the first observations to investigate spectral and compositional changes of heavy ions (carbon, oxygen, and iron) during ESP events (Klecker et al. 1981), showing that the Fe/O ratio decreases with time in ESP events.

Observations of ESP events at about 1 AU show that the particle intensity increases gradually prior to shock passage, peaking in intensity at the shock, with a characteristic time scale that increases with energy over $\sim 0.1$ hours at 30 keV to $\sim 10$ hours at 1 MeV (Klecker et al. 1981; Decker et al. 1981; Scholer and Ipavich 1983).

The shock acceleration process is the most important process for producing ESP enhancements (Scholer and Morfill 1975). Therefore we can apply a diffusive shock acceleration mechanism to study ESP events (e.g., Lee 1983; Baring et al. 1997).

## 2.4 Observation of Energetic Storm Particle Events

Observations of energetic storm particle (ESP) events from modern instruments on spacecraft (e.g., ACE, SOHO, Yohkoh, ISEE, WIND, etc.) provide detailed information on characteristics of IP shock passage, energy spectra of ESP, and mechanisms of shock acceleration of seed particles. These spacecraft observations are the only way to measure non-relativistic cosmic rays, which fragment in Earth's atmosphere.

An example of ESP observations from the ACE spacecraft at about 1 AU (near the Earth) is shown in Figure 2.5. This displays measurements during June 21 to June 26, 2000, including an ESP event, from the ACE spacecraft's Ultra

Low Energy Isotope Spectrometer (ULEIS) (Mason et al. 1998), Magnetometer (MAG) (Smith et al. 1998), and Solar Wind Electron, Proton and Alpha Monitor (SWEPAM) (Desai et al. 2003). We see changing energetic ion densities, magnetic field magnitude, and solar wind plasma speed at different times during the IP shock event.

The ACE observations clearly indicate the presence of ESP. When the IP shock reaches the ACE spacecraft we see a peak in particle intensity (e.g., He, O, or Fe ions), at 12:27 UT on June 23, 2000 (see Figure 2.5a; note that a convenient unit for energetic ion observations is the kinetic energy divided by mass number, $E/A$, expressed as MeV/nucleon, a quantity that depends only on velocity). This confirms the idea that the energetic particles are generated (accelerated) at the IP shock.

Note that the particle intensity gradually increases due to the IP shock passage (from 07:28 UT on June 22, 2000 to 00:24 UT on June 24, 2000) in the ESP event. We will explain such ACE observations with the finite time shock acceleration model (see Chapter 4). For the upstream seed particles (from 11:06 UT on June 20, 2000 to 05:48 UT on June 22, 2000) the particle intensity does not increase.

Figure 2.6 displays shock energy spectra of He, C, O, Fe from the ESP event of June 22-23, 2000 and the preceding upstream population from ULEIS observations on the ACE spacecraft. We see that shock spectra (Figure 2.6b) are changed from the upstream seed spectra (Figure 2.6a) due to the effect of shock acceleration of particles in IP space.

We found that the rollover energy in shock spectra (Figure 2.6b) occurs at about 0.1 to 5 MeV/nucleon. From characteristics of shock spectra (Figure

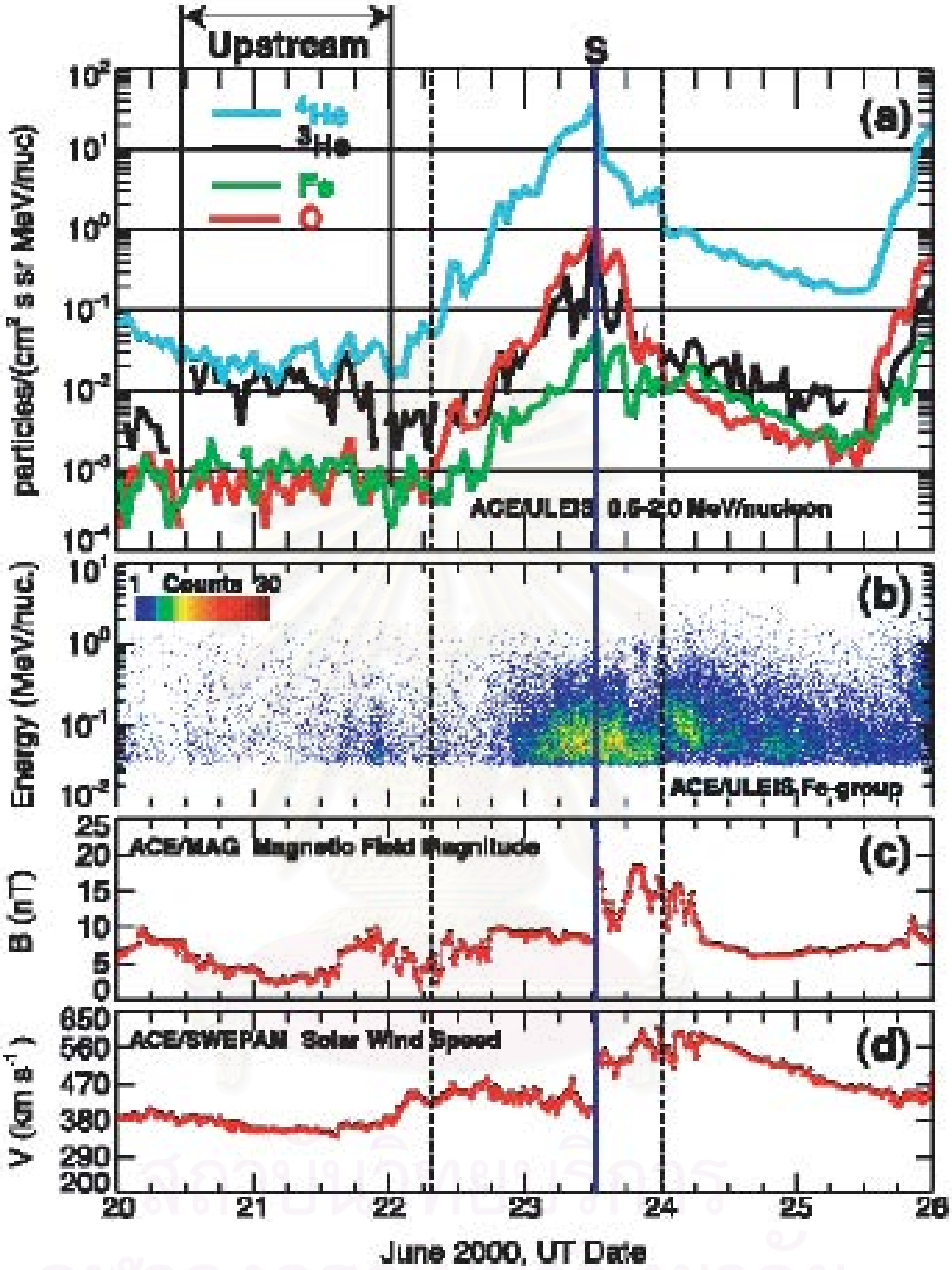


Figure 2.5: Observations of the ESP event on June 20-26, 2000 from the ACE spacecraft. (a) Intensity-time profiles of 0.5-2.0 MeV/nucleon $^3$He, $^4$He, O, and Fe ions. (b) Energy scatter plot of 0.03-3.0 MeV/nucleon Fe-group ions. (c) Magnetic field magnitude, $B$. (d) Solar wind speed, $V$. Vertical line labeled S marks the arrival of the interplanetary shock at ACE at 12:27 UT on June 23, 2000. Dashed vertical lines define the time interval assigned to ESP. (Picture credit: Desai et al. 2003)

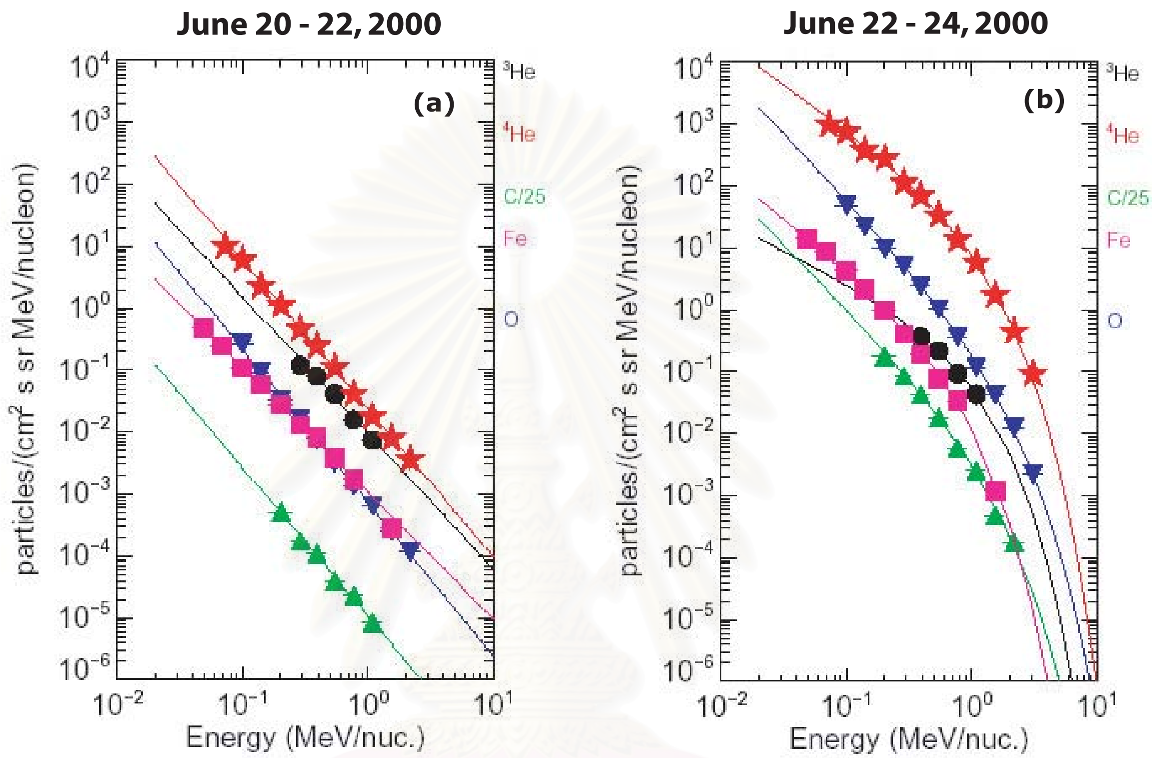


Figure 2.6: Energy spectra of $^3$He, $^4$He, C, O, and Fe ions from ULEIS observations. (a) Energy spectra before IP shock passage (upstream) in the time interval June 20-22, 2000, and (b) at IP shock passage in the time interval June 22-24, 2000 [*stars* for $^4$He, *circles* for $^3$He, *squares* for Fe, *triangles* for C, *inverted triangles* for O].

2.6b), Desai et al. (2004) fit observational data of IP shock acceleration in ESP events with the expression of Ellison and Ramaty (1985):

$$J(E) = J_0 E^{-\gamma} \exp(-E/E_c),$$

where $J(E)$ is the differential intensity vs. energy $E$, $J_0$ is a normalization constant, $\gamma$ is the spectral index (theoretically depending only on the shock compression ratio), and $E_c$ is a cut-off energy.

## 2.5 Astrophysical Shock Acceleration

Astrophysical shock waves are a subject of extensive space astrophysics research, especially with regard to high energy particles and the physics of particle acceleration, which are very important for understanding how charged particles can be accelerated to high energies.

Acceleration of energetic particles at shock waves occurs routinely in a variety of astrophysical situations such as inside our solar system, beyond the solar system, and even outside our galaxy. Particle acceleration can occur generically through interactions with a shock or plasma wave turbulences (Miller 1998).

Shock waves, or more simply, “shocks” are produced when a disturbance moves through a fluid faster than the characteristic speed of propagation of small amplitude waves in the medium (e.g., faster than the sound speed in an unmagnetized plasma, or faster than the Alfv́en speed in a magnetized plasma). Space is not empty, but rather filled with plasmas, so shocks are produced by collisionless plasmas. They are magnetohydrodynamic (MHD) shock waves.

For examples of astrophysical situations, shocks are produced by explosions in space (e.g., supernova explosions, solar flare eruptions, ejecta of CME traveling through IP space), or in general when a fluid moving faster than the relevant characteristic speed encounters a slower-moving fluid, such as the solar wind collision with the interstellar medium at the termination shock, the bow shock of Earth's magnetosphere, etc. Shocks may also be produced when a wave encounters a region where the local characteristic speed decreases in the direction of propagation of the wave.

At a shock front, fluid parameters (e.g., velocity, pressure, density, and magnetic field) change discontinuously, because the fluid ahead of the shock can have no warning of the shock's approach.

Mechanisms of shock acceleration of charged particles in astrophysical space have been described for many years (Parker 1958a; Krymskii 1977; Axford, Leer, and Skadron 1977; Bell 1978a, 1978b; Blanford and Ostriker 1978; Drury 1983) based on the original first-order Fermi acceleration mechanism (Fermi 1954). There seems to be a consensus that cosmic rays with energy up to $10^6$ GeV/nucleon (Lagage and Cesarsky 1983a, 1983b; Achterberg 1988; Prothroe 1996) can be accelerated by supernova remnants (SNR) in our galaxy.

### 2.5.1 Fermi Acceleration Mechanism

Fermi (1949) presented the concept of the mechanism of particle acceleration in space plasmas to explain the origin of high energy particles in interstellar space (cosmic rays). Consider charged particles colliding with a huge magnetic cloud moving in interstellar space. If such clouds have irregular directions of motion in the interstellar medium, the different rates of "head-on" and "following" collisions between the charged particles and the magnetic clouds would lead to net acceleration.

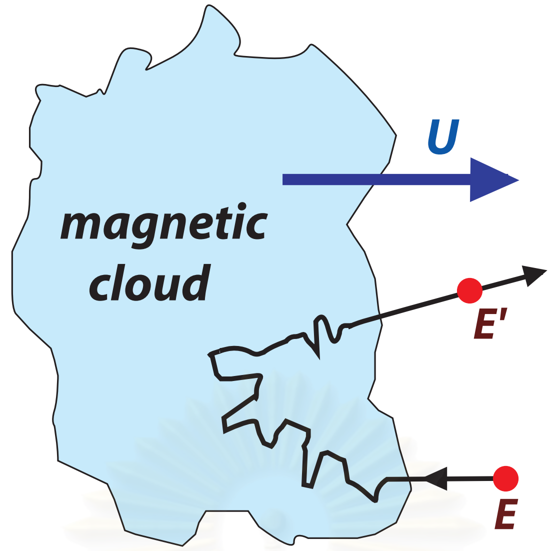


Figure 2.7: Second-order Fermi acceleration: A particle is reflected by scattering in a magnetic cloud. The net result is a "collision" with the cloud.

The motion of a particle scattered by random magnetic field irregularities inside the cloud can be considered a random walk (see Figure 2.7, which shows a single collision of a particle with the magnetic cloud).

The probabilities of head-on and following collisions are proportional to the relative velocities of approach of the particle and the magnetic cloud (Longair 1994). The probability of a head-on collision is $v + U\cos\theta$, and for a following collision is $v - U\cos\theta$, where $v$ is the velocity of the particle, $U$ is the velocity of the magnetized cloud, and $\theta$ is the collision angle. The probability of a head-on collision is higher than a following collision, hence on average a particle gains energy. Assuming the particle to be relativistic ($E \approx pc$), the net energy gain (average per collision) is

$$\left\langle \frac{\Delta E}{E} \right\rangle \approx \frac{4}{3}\left(\frac{U}{c}\right)^2 \tag{2.1}$$

where $c$ is the velocity of light (Protheroe 1996; Usoskin and Mursula 2001).

The result from the acceleration mechanism in (2.1) is an energy increase only to second order in $U/c$. Thus the model of Fermi (1949) was known as the "second-order Fermi acceleration mechanism."

Gas clouds in the interstellar medium have random velocities of about $U = 15$ km/s (Protheroe 1996). Thus $U \ll c$, and this acceleration process is slow. This process is used to describe the interaction between high energy particles and waves or irregularities in the interstellar magnetic field, by which particles gain energy by being scattered stochastically off plasma waves (Longair 1994). Anyway, this theory cannot completely explain the energy spectrum of galactic cosmic rays from observations.

Fermi (1954) proposed a new concept for a faster, first-order acceleration mechanism for charged particles at magneto-hydrodynamic shocks (de Hoffman and Teller 1950). At a shock front there are sudden variations, effectively a discontinuity, in direction and intensity of the magnetic field. There can be collisions between charged particles and magnetic field irregularities in the "upstream" region (ahead of the shock front) and "downstream" region (behind the shock front) (see Figure 2.8). A charged particle at the upstream side can pass through the shock and then be scattered by magnetic inhomogeneities downstream.

The results from this mechanism indicate that particles can gain energy per cycle more efficiently than for the Fermi(1949) mechanism. The energy of particle crossing the shock is

$$\frac{\Delta E}{E} \approx \frac{4}{3}\left(\frac{V_{shock}}{c}\right) \tag{2.2}$$

where $c$ is velocity of light, and $V_{shock}$ is velocity of the shock front (Longair 1994;

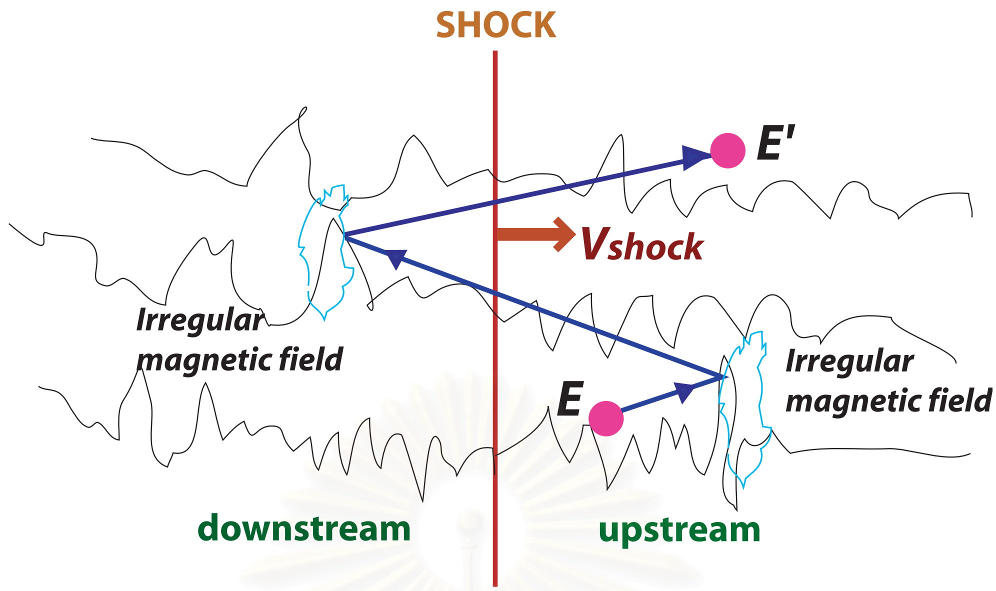


Figure 2.8: First order Fermi acceleration: Interaction of a particle of energy $E$ with a shock moving with speed $V_{shock}$.

Protheroe 1996; Usoskin and Mursula 2001). This theory is known as the "first-order Fermi acceleration mechanism." The first-order Fermi acceleration has been used to explain galactic cosmic ray and solar energetic particle acceleration (Jones and Ellison 1991; Reames 1999).

This theory completely explains the energy spectrum of galactic cosmic ray up to $\sim 10^{14}$ eV. The power-law momentum distribution of cosmic rays corresponds to real observations of cosmic ray intensity (Kryskii 1977; Bell 1978; Blandford and Ostriker 1978; Axford 1981; Kirk and Dendy 2001).

### 2.5.2 Diffusive Shock Acceleration

Diffusive shock acceleration (DSA) is generally thought to be the key mechanism to explain the acceleration of charged energetic particles diffusing in astrophysical space (Drury 1983; Lagage and Cesarsky 1983b; Jokipii 1987; Jones and Ellision

1991; Kirk and Dendy 2001). The concept of DSA is based on the first-order Fermi shock acceleration mechanism (Fermi 1954), mentioned in section 2.5.1. The DSA mechanism concerns acceleration in which charged particles repeatedly scatter on irregularities of the magnetic field on two sides of the shock wave (multiple shock encounters).

We know that space plasmas almost always have a variety of magnetic field irregularities. This causes energetic charged particles to scatter in pitch angle and change their direction. This phenomenon leads to a diffusion process in space, and is the basis of the DSA idea. The process of DSA refers to the acceleration of charged particles as they are repeatedly scattered back and forth across the shock front (a thin region with a discontinuity of fluid plasma speed and magnetic field intensity) along the direction of the magnetic field (Figure 2.9). The diffusion process can be viewed as a "collision" between the charged particle and macroscopic magnetic field irregularities (Krymskii 1977; Drury 1983). Such magnetic field irregularities flow with the fluid plasma speed. If a particle is bouncing back and forth across the shock on the "upstream" side it undergoes a head-on collision and gains energy, while a particle bouncing back and forth across the shock on the "downstream" side undergoes a following collision and loses energy. In a complete cycle of a particle crossing a shock by bouncing back and forth, a particle will gain more energy than it loses. The reason is because roughly speaking the speed increases by $2U_1$ upstream and decreases by $2U_2$ downstream. From the fundamental physics of the shock, $U_1 > U_2$; therefore, a net result is energy gain or momentum gain. For a non-relativistic particle, the mean momentum gain ($\Delta p$) per cycle is about

$$\Delta p \approx 2m(U_1 - U_2)$$

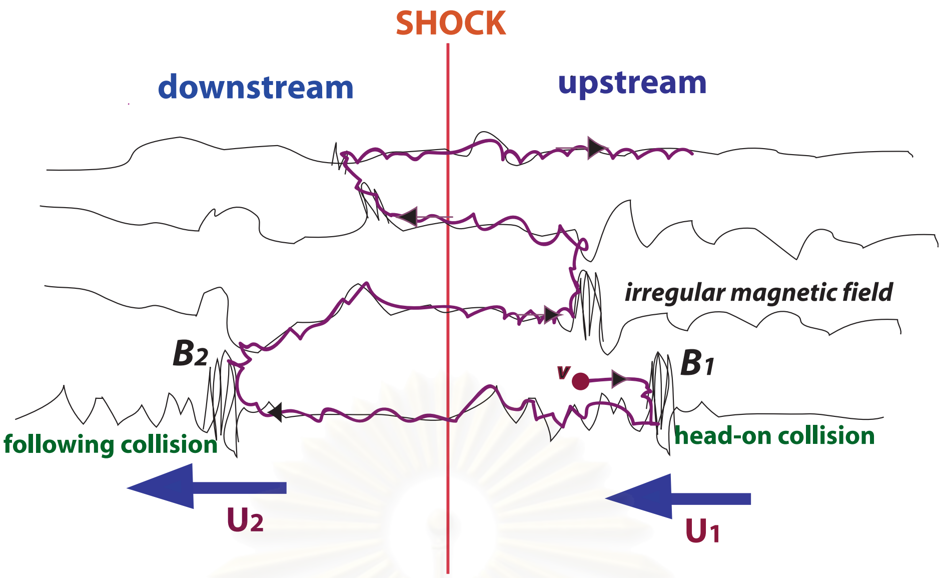


Figure 2.9: Diffusive shock acceleration. In the shock frame, a charged particle diffuses due to motion along an irregular magnetic field that results in repeated motion (diffusion) back and forth across the shock wave. Upstream, a charged particle collides with the irregular magnetic field ($B_1$) by a head-on collision. Downstream, a charged particle collides with the irregular magnetic field ($B_2$) by a following collision.

We see that the relative momentum gain for a cycle of two crossings of the shock is then proportional to the velocity difference across the shock.

Drury (1983) considered a particle to have momentum, $p$, velocity, $v$, and pitch angle, $\mu = \cos\theta$, in the upstream fluid frame. Suppose that the magnetic field $\vec{B}$ points along the shock normal $\hat{n}$. Then in the shock frame the particle momentum is $p(1+\mu U_1/v)$. This is unchanged when crossing the shock, so relative to the downstream fluid frame its momentum is $p(1+\mu(U_1-U_2)/v)$. To order $U/v$ we can ignore the small changes in pitch angle as we change from frame to frame and also the anisotropy in the directional distribution when averaging. (These effects are taken into account by Ruffolo 1999.) Thus the average change in momentum is

$$\langle \Delta p \rangle = p \int_0^1 [\mu (U_1 - U_2)/v] \; 2\mu d\mu \tag{2.3}$$

$$\langle \Delta p \rangle = \frac{2}{3} \frac{U_1 - U_2}{v} p. \tag{2.4}$$

For a complete cycle (from upstream to downstream and returning upstream) we get

$$\langle \Delta p \rangle = \frac{4}{3} \frac{U_1 - U_2}{v} p \tag{2.5}$$

(Drury 1983; Kirk 1994).

The general process of charged particle acceleration by DSA can also be described by the evolution of the particle distribution function, $f(\mathbf{r}, \mathbf{p}, t)$, as a function of position $\mathbf{r}$, particle momentum $p$, and time $t$ in terms of the diffusion-convection equation (e.g., Parker 1965; Axford et al. 1977; Krymskii 1977; Bell 1978a; Blandford and Ostriker 1978; Forman 1981; Drury 1983)

$$\frac{\partial f(\mathbf{r}, \mathbf{p}, t)}{\partial t} + \mathbf{U} \cdot \nabla f(\mathbf{r}, \mathbf{p}, t) - \nabla \cdot [k \nabla f(\mathbf{r}, \mathbf{p}, t)] - \frac{\nabla \cdot \mathbf{U}}{3} \, p \frac{\partial f(\mathbf{r}, \mathbf{p}, t)}{\partial p} = 0. \tag{2.6}$$

In equation (2.6), $p$ is the particle momentum, $k$ is the diffusion coefficient in the background plasma, and $U$ is the velocity of the fluid background plasma (Forman 1981). Equation (2.6) is considered in the shock frame.

Consider equation (2.6) in 1-dimensional space (along the x-axis). In this frame the shock wave is stationary. Then for a steady state, $\partial f / \partial t = 0$ and we write

$$\frac{\partial}{\partial x} \left[ U f(x,p) - k \frac{\partial f(x,p)}{\partial x} \right] - \frac{1}{3} \left( \frac{\partial U}{\partial x} \right) \frac{\partial}{\partial p} [p f(x,p)] = 0. \tag{2.7}$$

At the shock front there is a discontinuity in the velocity of the fluid. When we consider the shock frame, then there are 2 regions separated by the

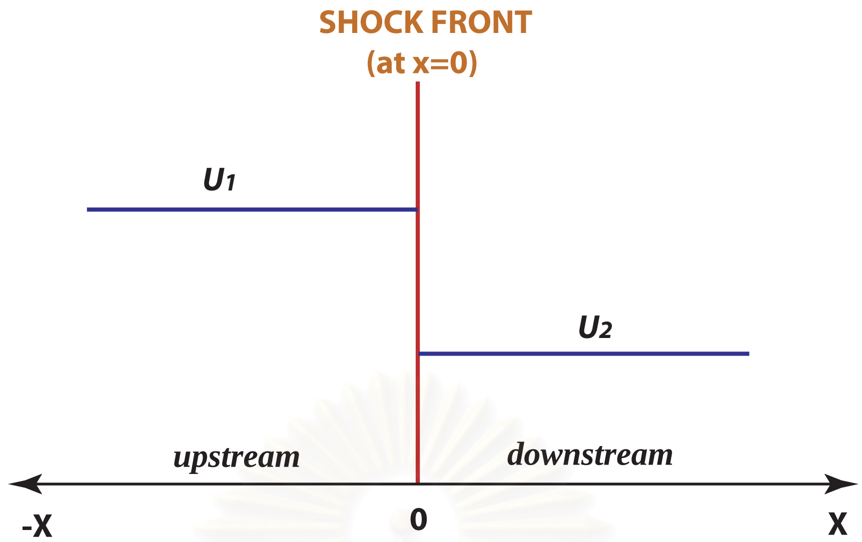


Figure 2.10: Fluid speed $U(x)$ on the upstream and downstream sides when considering a discontinuity at the shock.

shock front: the upstream side ($x < 0$) and downstream side ($x > 0$). Therefore the velocity of the fluid plasma is (see Figure 2.10)

$$U(x) = \begin{cases} U_1 & \text{for} \quad x < 0 \quad \text{(upstream side)} \\ U_2 & \text{for} \quad x > 0 \quad \text{(downstream side).} \end{cases}$$

Thus we get

$$\frac{\partial}{\partial x}\left[Uf(x,p) - k\frac{\partial f(x,p)}{\partial x}\right] - \frac{1}{3}(U_2 - U_1)\delta(x)\frac{\partial}{\partial p}[pf(x,p)] = 0. \tag{2.8}$$

We have $\partial U/\partial x$ in the regions where $x \neq 0$, i.e., either $x < 0$ or $x > 0$. Thus according to (2.8), the particle flux must be constant on either side of the shock:

$$\frac{\partial}{\partial x}\left[Uf(x,p) - k\frac{\partial f(x,p)}{\partial x}\right] = 0 \tag{2.9}$$

$$Uf(x,p) - k\frac{\partial f(x,p)}{\partial x} = \text{Constant} \quad (\text{in } x). \tag{2.10}$$

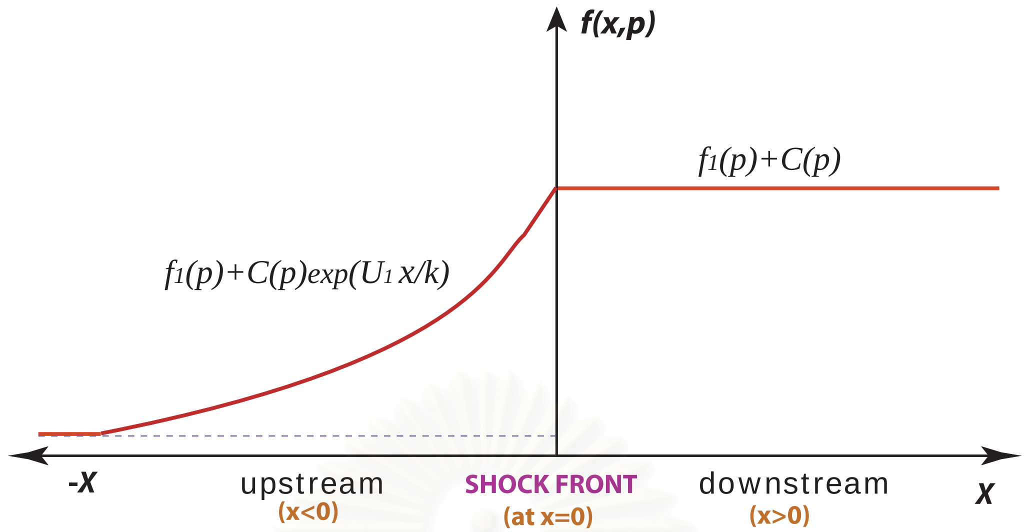


Figure 2.11: Solution $f(x,p)$ of the steady-state diffusive shock acceleration model upstream and downstream of the shock.

We get the general solution

$$f(x,p) = C(p)\exp\left(\int_0^x \frac{U(x')}{k(x')}dx'\right) + D(p), \tag{2.11}$$

where $C$ and $D$ are arbitrary functions of $p$.

When considering the boundary condition in the region of the shock where particles flow into the shock from far upstream ($x \to -\infty$), we set $f(x = -\infty, p) = f_1(p)$. On the downstream side ($0 < x < \infty$), $f(x,p)$ does not depend on distance. Thus

$$f(x,p) = \begin{cases} f_1(p) + C(p)\exp(U_1 x/k) & x < 0 \quad \text{(upstream side)} \\ f_2(p) & x > 0 \quad \text{(downstream side).} \end{cases} \tag{2.12}$$

If functions $f_1(p)$, $f_2(p)$, and $C(p)$ match at the shock front ($x$=0),

$$f(x = 0, p) = f_2(p) = f_1(p) + C(p),$$

then

$$f(x,p) = \begin{cases} f_1(p) + C(p)\exp(U_1 x/k) & x < 0 \quad \text{(upstream side)} \\ f_1(p) + C(p) & x \geq 0 \quad \text{(downstream side).} \end{cases} \tag{2.13}$$

The solution $f(x,p)$ is shown as a function of $x$ in Figure 2.11. Actually, Drury (1983), Ruffolo (1999), and Gieseler et al. (1999) suggested that the condition in (2.12) may involve a mismatch to order $O(U/v)$.

Next we consider the solution in momentum space at the shock front and the downstream side where $f(x,p)$ is constant for $x \geq 0$, i.e., $f(x \geq 0, p) = f_2(p)$. In this case, we can derive the distribution function of momentum that results from shock acceleration processes observed in the region behind the shock front. Consider the discontinuity at the shock front, by integrating equation (2.8) over $-\epsilon \to \epsilon$, where $\epsilon$ is very small. The net outflow of particles from the shock is in the downstream direction. The flux of particles in this case (at the shock front) is $U_2 f_2(p)$:

$$\frac{1}{3}(U_2 - U_1)\frac{\partial}{\partial p}[p f_2(p)] = U_2 f_2(p) \tag{2.14}$$

$$\frac{\partial}{\partial p}[p f_2(p)] = \frac{3U_2}{U_1 - U_2} f_2(p). \tag{2.15}$$

Therefore we get the solution

$$f_2(p) = A p^{-3U_2/(U_1-U_2)-1} \tag{2.16}$$

(Kirk 1994) where $A$ is a constant.

Considering the shock compression ratio $r = U_1/U_2$,

$$f_2(p) = A p^{-[(r+2)/(r-1)]}, \tag{2.17}$$

which we can write in the form

$$f_2(p) = A p^{-\gamma}, \tag{2.18}$$

where $\gamma$ is a power-law spectral index, $\gamma = (r+2)/(r-1)$. Therefore, the result from DSA can yield a power-law momentum spectrum of the accelerated particle population with spectral index, $\gamma$.

For the strong shock case, $r = U_1/U_2 = 4$ (e.g., Krymskii 1977; Lagage and Cesarsky 1983a; Ruffolo 1999; Kirk and Dendy 2001). Then the particle distribution function $f_2(p) \approx p^{-2}$ is very close to the observed momentum and energy spectrum of high energy cosmic rays ($10^5 - 10^{15}$ eV) that are accelerated by strong SNR shocks (Kryskii 1977; Bell 1978a, 1978b; Blandford and Ostriker 1978; Axford 1981; Lagage and Cesarsky 1983a; Kirk and Dendy 2001).

# CHAPTER III

# FINITE TIME SHOCK ACCELERATION

Observations of energetic ion acceleration at interplanetary (IP) shocks by spacecraft instruments often indicate a spectral rollover of energy [at above 0.2 MeV, Gosling et al. (1981); $\sim$ 0.2 to 1 MeV, van Nes et al. (1985); $\sim$0.2 to 5 MeV/nucleon, Desai et al. (2004)]. This rollover is not well explained by a finite shock width effect (Ellison and Ramaty 1985), which does not apply to a shock of extended width. The drift effect over the shock width gives a rollover energy that is too high (energy per charge larger than 100 MeV/$Q$). At the same time, a typical timescale of diffusive shock acceleration is several days, implying that the process of shock acceleration at an IP shocks near Earth usually gives only a mild increase in energy to an existing seed particle population, which is consistent with a recent analysis of ULEIS observations (Desai et al. 2003, 2004) that argues for a seed population at substantially higher energies than the solar wind. Therefore an explanation of typical spectra of IP shock-accelerated ions requires a model of finite-time shock acceleration (e.g., Ruffolo and Channok 2003; Channok et al. 2004).

We model finite-time shock acceleration (FTSA) from a probability approach (Bell 1978a; Drury 1983). In the situation of a shock acceleration process in which particles move across the shock between upstream and downstream of the shock, some particles are accelerated and then move across the shock again, and some particles can escape from the shock.

In this chapter we formulate and derive analytical and numerical expression for our FTSA model for simulation of shock acceleration of seed ions at IP shocks, to describe energy spectra of energetic storm particle events in observational data from the ULEIS instrument (Mason et al. 1998)on the ACE spacecraft.

## 3.1 Physical Situation

In the situation of interest, we focus on energetic storm particle events in which seed energetic particles are accelerated by IP shocks in the IP medium (see Figure 3.1a). An IP shock moving out from the Sun (driven by a CME) with high speed in IP space then later accelerates a seed SEPs population in the upstream region.

We consider that at the shock front there are discontinuous changes from upstream to downstream, where the IP magnetic field line changes in intensity from $|\vec{B}_1|$ to $|\vec{B}_2|$ and in direction with respect to the shock normal from $\theta_1$ to $\theta_2$ (Figure 3.1). We consider the reference frame in which the fluid plasma flows along magnetic field lines (Figure 3.1b) so that $\vec{U}||\vec{B}$. This is called the de Hoffman-Teller frame (de Hoffman and Teller 1950; Bell 1978a; Ruffolo 1999). We model the shock structure as a planar shock (Figure 3.1b) known as an oblique shock, i.e., with $\theta_1$ between 0 and 90 degrees. On the upstream side we have magnetic field $\vec{B}_1$ and plasma speed $\vec{U}_1$, and the angle between $\vec{B}_1$ and the shock normal ($\hat{n}$) is the upsteam shock angle $\theta_1$, also known as $\theta_{Bn}$ (Desai et al. 2003,

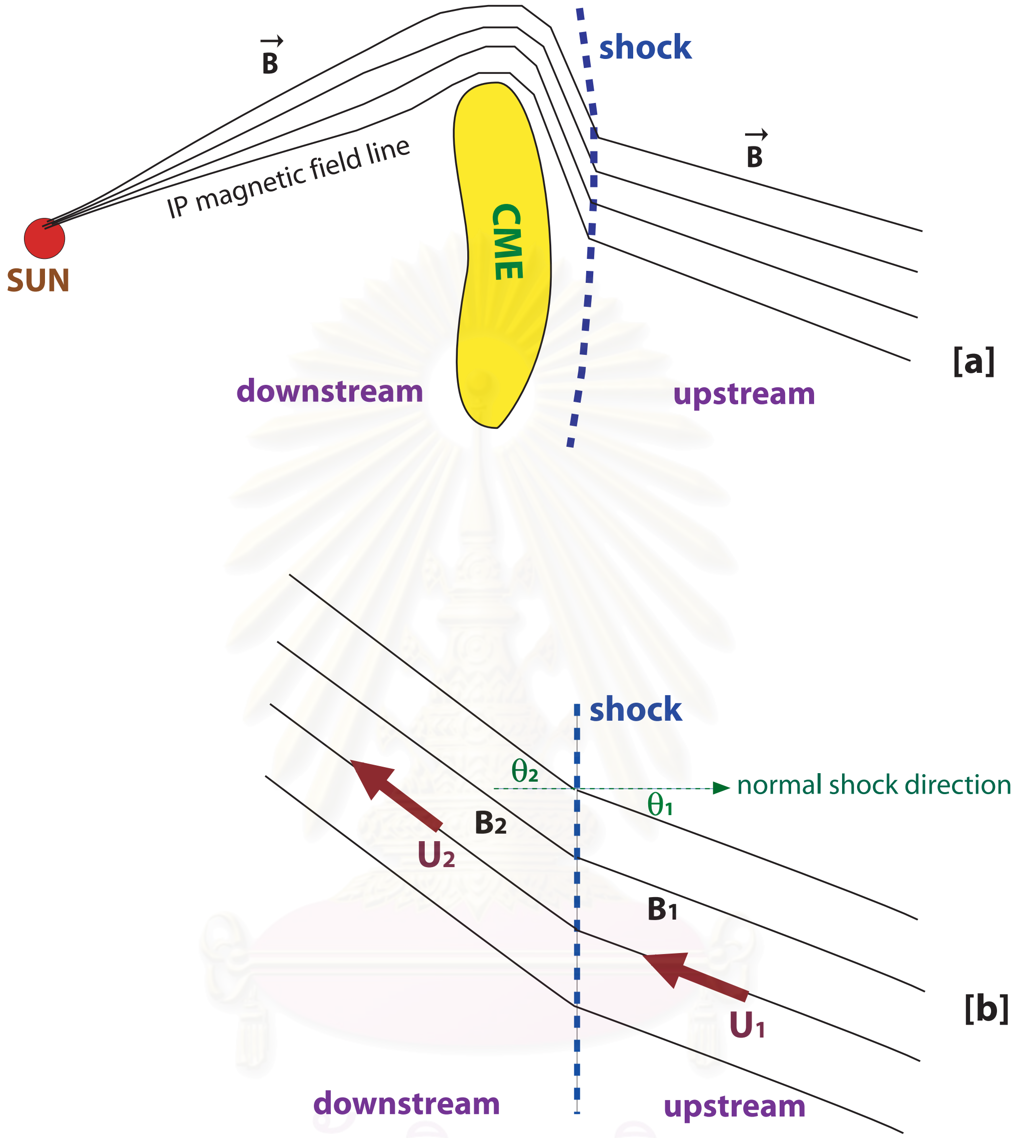


Figure 3.1: (a) Situation of interplanetary shock acceleration by a coronal mass ejection (CME) shock. (b) Our model of an oblique shock for study in this work to consider characteristics of $\vec{B}$ and $\vec{U}$ in the shock frame.

2004). The downstream side has magnetic field $\vec{B}_2$ and plasma fluid speed $\vec{U}_2$, and the angle between $\vec{B}_2$ and the shock normal ($\hat{n}$) is the downstream shock angle $\theta_2$. The unit shock normal direction ($\hat{n}$) can be determined from just two measurements of $\vec{B}$, upstream and downstream:

$$\hat{n} = \frac{(\vec{B}_1 \times \vec{B}_2) \times (\vec{B}_1 - \vec{B}_2)}{|(\vec{B}_1 \times \vec{B}_2) \times (\vec{B}_1 - \vec{B}_2)|}$$

(Colburn and Solnett 1966; Abraham-Shrauner 1972; Burlaga 1995).

Consider particle acceleration at the shock with the shock parameters $B_1$ and $\theta_1$ (upstream) and $B_2$ and $\theta_2$ (downstream). The relation between $B_1$, $B_2$, $\theta_1$, and $\theta_2$ is

$$\frac{B_2}{B_1} = \sqrt{\frac{B_{2x}^2 + B_{2y}^2}{B_{1x}^2 + B_{1y}^2}} = \sqrt{\frac{1+\tan^2\theta_2}{1+\tan^2\theta_1}} = \frac{\sec\theta_2}{\sec\theta_1} \tag{3.1}$$

[derived by Burlaga (1995) and Ruffolo (1999)].

The mean momentum gain when a particle moves across the shock for one cycle (from upstream to downstream and returning to upstream; see Figure 3.2) is given by

$$p_1 = p_0 + \frac{4}{3}\frac{U_1\cos\theta_1 - U_2\cos\theta_2}{v_0\cos\theta_1}\,p_0, \tag{3.2}$$

where $p_0$ is the initial particle momentum, $p_1$ is the particle momentum after one cycle of acceleration, and $v_0$ is the initial particle velocity (derived by Drury 1983).

When a particle moves across the shock for $n$ cycles (or $n$ times), the average particle momentum is

$$p_n \approx \prod_{i=1}^{n}\left(1 + \frac{4}{3}\frac{U_1\cos\theta_1 - U_2\cos\theta_2}{v_i\cos\theta_1}\right)p_0, \tag{3.3}$$

where $v_i$ is the particle velocity after $i$ crossings.

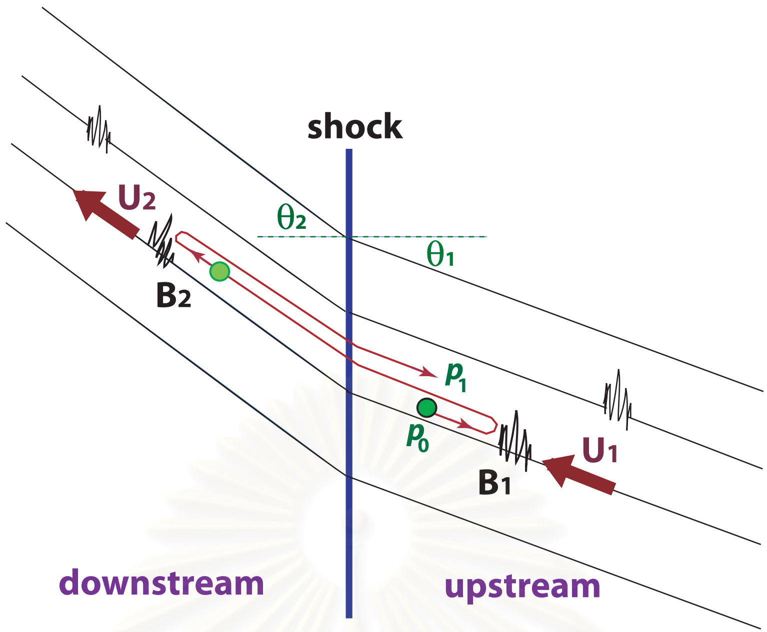


Figure 3.2: Acceleration of a particle crossing the shock for one cycle. The particle momentum increases from $p_0$ to $p_1$.

In our model we use $u_1$ to mean the component of the upstream velocity in the direction of the shock normal, so $u_1 = U_{1n} = U_1 \cos\theta_1$, and $u_2$ is the normal velocity downstream, $u_2 = U_{2n} = U_2 \cos\theta_2$. We use values $u_1$ and $u_2$ that correspond to spacecraft observations (Desai et al. 2004) of plasma fluid speed along the shock normal.

We write momentum of a particle crossing the shock $n$ times as

$$p_n = p_{n-1} + \frac{4}{3}\frac{(u_1 - u_2)}{v_{n-1}\cos\theta_1} p_{n-1}. \tag{3.4}$$

From (3.4) we can calculate the kinetic energy ($E$) of a particle that crosses the shock $n$ times, $E_n$, from the corresponding $p_n$.

The time for acceleration, $T_{acc}$, of particles from an initial momentum $p_0$

to a momentum $p_n$, for a parallel shock, can be written as

$$T_{acc} = \frac{3}{u_1 - u_2} \int_{p_0}^{p_n} \left( \frac{\kappa_1 \sec\theta_1}{u_1} + \frac{\kappa_2 \sec\theta_2}{u_2} \right) \frac{dp}{p}$$

(Forman and Morfill 1979; Drury 1983; Jokipii 1987; Kallenrode 2001), where $\kappa_1$ is the upstream diffusion coefficient along the shock normal, and $\kappa_2$ is the downstream diffusion coefficient along the shock normal.

For an oblique shock, some particles are reflected due to the magnetic field change at the shock front, and some particles are transmitted downstream.

Consider the adiabatic invariant at the shock in which a magetic moment is approximately conserved (Terasawa 1979):

$$\begin{aligned} \frac{p_1^2 \sin^2\theta_1}{B_1} &= \frac{p_1^2 \sin^2\theta_2}{B_2} \\ \frac{1 - \cos^2\theta_1}{B_1} &= \frac{1 - \cos^2\theta_2}{B_2}. \end{aligned}$$

Particles are transmitted downstream only when $\cos^2\theta_2$ has a physical value ($\cos^2\theta_2 > 0$), i.e., when $\cos\theta_1 > \sqrt{1 - (B_1/B_2)}$. Since the particle distribution is nearly isotropic, i.e., uniform in $\cos\theta_1$, the transmission probability among particles moving toward the shock is $1 - \sqrt{1 - B_1/B_2}$.

We introduce a new formula that takes this reflection probability into account:

$$T_{acc} = \frac{3}{u_1 - u_2} \int_{p_0}^{p_n} \left\{ \frac{\kappa_1 \sec\theta_1}{u_1} + [1 - \sqrt{1 - (B_1/B_2)}] \frac{\kappa_2 \sec\theta_2}{u_2} \right\} \frac{dp}{p}.$$

## 3.2 FTSA Formulation

We further develop the finite-time shock acceleration (FTSA) model following the preliminary report of Ruffolo and Channok (2003). We employ a probabilistic approach following the theory of Bell (1978a) and Drury (1983). The key concept of shock acceleration of charged particles is that a particle has a certain probability of escape after each acceleration event, so that only some of the particles reach higher energies.

In the diffusive shock acceleration process by which particles move across the shock between upstream and downstream over a time interval $t$, some particles are accelerated then return to the shock again and some particles escape from the shock (Bell 1978a). The model only considers escape downstream, on the basis that convection would eventually bring upstream particles back to the shock.

We consider a particle moving cross the shock for one cycle, and then in the next step we consider the probability that a particle will move across the shock again, or the probability that a particle will escape from the shock (with no further acceleration). The key parameters in this model are the acceleration rate ($r$) and escape rate ($\epsilon$).

### 3.2.1 Analytical Model

We consider shock acceleration events over the residence time $T$ over which a particle is in the acceleration region. We can use a simple parameter to describe the behavior of particle acceleration at the shock with the acceleration rate,

$$r = 1/\Delta t, \tag{3.5}$$

where $\Delta t$ is time that a particle takes to diffuse across the shock for one cycle (from upstream to downstream and returning from downstream to upstream):

$$\Delta t = \frac{4}{v}\left\{\frac{\kappa_1 \sec\theta_1}{u_1} + [1 - \sqrt{1-(B_1/B_2)}]\frac{\kappa_2 \sec\theta_2}{u_2}\right\}, \tag{3.6}$$

where $v$ is the particle velocity, $u_1$ is the upstream fluid speed, $\theta_1$ is the field-shock normal angle upstream, $\kappa_1$ is the diffusion coefficient upstream, $B_1$ is the average magnetic field intensity upstream, $u_2$ is the downstream fluid speed, $\theta_2$ is the field-shock normal angle downstream, $\kappa_2$ is the diffusion coefficient downstream, and $B_2$ is the average magnetic field intensity downstream. Note that $u_1, u_2, \kappa_1$, and $\kappa_2$ are values in the shock normal direction. We do not yet consider adiabatic deceleration at this point. We introduce the term $1 - \sqrt{1 - (B_1/B_2)}$ in equation (3.6) as the probability of transmission of particles through the IP shock along the magnetic field.

We define the Poisson distribution of the number of acceleration events $n$ during a residence time $T$ as

$$P(n, T) = \frac{(rT)^n}{n!} \exp(-rT). \tag{3.7}$$

We also consider the number of particles remaining in the shock acceleration region after residence time $T$ with escape rate, $\epsilon$. We construct a function of the distribution of residence times composed of an initial term and an inflow term. In this function we consider the residence time, $T$, and the total duration, $t$:

$$N(T; t) = I \exp(-\epsilon T) + N_0 \exp(-\epsilon t)\delta(T - t), \tag{3.8}$$

where $I$ is the inflow function, and $N_0$ is the initial particle density at the shock. The first term is the inflow term. Some of those particles escape from the shock; therefore, this term decreases with residence time $T$. The second term is a function of the total time, $t$, at the shock.

The function $N(T; t)$ satisfies the following partial differential equation:

$$\frac{\partial N}{\partial t} + \frac{\partial N}{\partial T} + \epsilon N = 0.$$

The distribution function of particles $N(T; t)$ versus $T$ is shown in Figure 3.3.

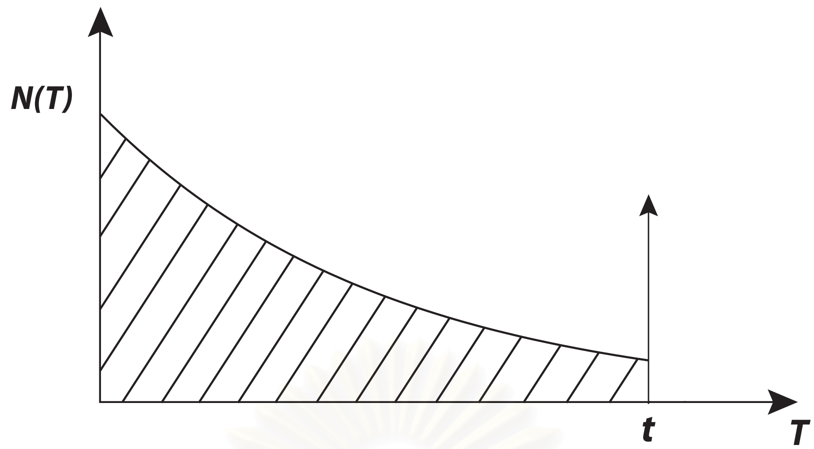


Figure 3.3: Model distribution function $N(T;t)$ for the residence time $T$, which can be no larger than the total time $t$ ($T \leq t$).

The escape rate, $\epsilon$, can be derived from the probability of particle escape from the shock (Bell 1978a; Drury 1983; Protheroe 1996) to lowest order in $(u/v)$ as

$$\text{probability of escape} = \frac{\epsilon}{r+\epsilon} = \frac{4u_2}{v\cos\theta_1}.$$

Here, we consider in more detail the effects of streaming and convection of the particles upstream of the shock.

The probability of escape is defined by the flux of particle loss downstream per flux of particles crossing from upstream to downstream.

The flux of particle loss downstream is

$$F_{\text{loss}} = nu_2$$

(Bell 1978a; Drury 1983; Protheroe 1996). The flux of particles crossing from upstream to downstream is

$$F_{\text{cross}} = \frac{n}{2}\int_{-u_1/v\cos\theta_1}^{1}(u_1 + v\cos\theta\cos\theta_1)d(\cos\theta)$$

$$
\begin{aligned}
&= \frac{n}{2}\int_{-u_1/v\cos\theta_1}^{1}(u_1+\mu v\cos\theta_1)d\mu \\
&= \frac{n}{2}\Big[u_1+\frac{v\cos\theta_1}{2}+\frac{u_1^2}{2v\cos\theta_1}\Big] \\
&= n\Big[\frac{u_1}{2}+\frac{v\cos\theta_1}{4}+\frac{u_1^2}{4v\cos\theta_1}\Big].
\end{aligned}
$$

What is new here is the lower limit of integration, taking convection into account.

Thus we get the probability of particle escape as

$$
\begin{aligned}
\frac{\epsilon}{r+\epsilon} &= \frac{nu_2}{n\Big[\frac{u_1}{2}+\frac{v\cos\theta_1}{4}+\frac{u_1^2}{4v\cos\theta_1}\Big]} \\
\frac{\epsilon}{r+\epsilon} &= \frac{4u_2}{v\cos\theta_1[1+u_1/v\cos\theta_1]^2}.
\end{aligned}
$$

Then

$$
\frac{1}{\epsilon}=\Big[\frac{v\cos\theta_1}{4u_2}\Big(1+\frac{u_1}{v\cos\theta_1}\Big)^2-1\Big]\frac{1}{r},
$$

where $r$ does not include the effect of adiabatic deceleration.

Using (3.5) and (3.6), we then get a new formula for the escape rate as

$$
\epsilon=\left(\frac{4}{v}\Big[\frac{v\cos\theta_1}{4u_2}\Big(1+\frac{u_1}{v\cos\theta_1}\Big)^2-1\Big]\Big\{\frac{\kappa_1\sec\theta_1}{u_1}+[1-\sqrt{1-(B_1/B_2)}]\frac{\kappa_2\sec\theta_2}{u_2}\Big\}\right)^{-1}. \tag{3.9}
$$

- **Consider that $r$ and $\epsilon$ are constant**

We formulate an analytical model as a combinatorial model of finite-time shock acceleration by starting with a simple case by assuming a constant $r$ and a constant $\epsilon$ at any energy and at any time. We consider the process where particles are accelerated by the shock as in equation (3.7) and the distribution of residence times at the shock from the inflow term and initial term as in equation (3.8). We derive the overall distribution of particles with $n$ acceleration events at time $t$ as

$$N(n,t) = \int_0^t P(n,T)N(T;t)dT. \tag{3.10}$$

From equations (3.7) and (3.8) we get

$$\begin{aligned}
N(n,t) &= \int_0^t \frac{(rT)^n e^{-rT}}{n!} \cdot \Big(Ie^{-\epsilon T} + N_0 e^{-\epsilon t}\delta(T-t)\Big) dT \\
&= \int_0^t \frac{(rT)^n e^{-rT}}{n!} \cdot Ie^{-\epsilon T} dT + \int_0^t \frac{(rT)^n e^{-rT}}{n!} \cdot N_0 e^{-\epsilon t}\delta(T-t) dT \\
&= \frac{I}{n!}\int_0^t (rT)^n e^{-(r+\epsilon)T} dT + \frac{N_0}{n!} e^{-\epsilon t} \int_0^t e^{rT}(rT)^n \delta(T-t) dT \\
&= \frac{I}{n!} \cdot \frac{n!\ r^n}{(r+\epsilon)^{n+1}} \Big[1 - e^{-(r+\epsilon)t} \sum_{k=0}^{n} \frac{[(r+\epsilon)t]^k}{k!}\Big] + \frac{N_0}{n!} e^{-(r+\epsilon)t} \cdot (rt)^n.
\end{aligned}$$

Therefore the solution $N(n,t)$ in this case is

$$N(n,t) = I \cdot \frac{r^n}{(r+\epsilon)^{n+1}} \Big[1 - e^{-(r+\epsilon)t} \sum_{k=0}^{n} \frac{[(r+\epsilon)t]^k}{k!}\Big] + \frac{N_0}{n!} e^{-(r+\epsilon)t} (rt)^n, \tag{3.11}$$

where $N_0$ is the initial condition, $N_0(n) = N(n, t = 0)$. The analytical solution in (3.11) can be used for the case when $r$ and $\epsilon$ are constant (see Figure 3.4).

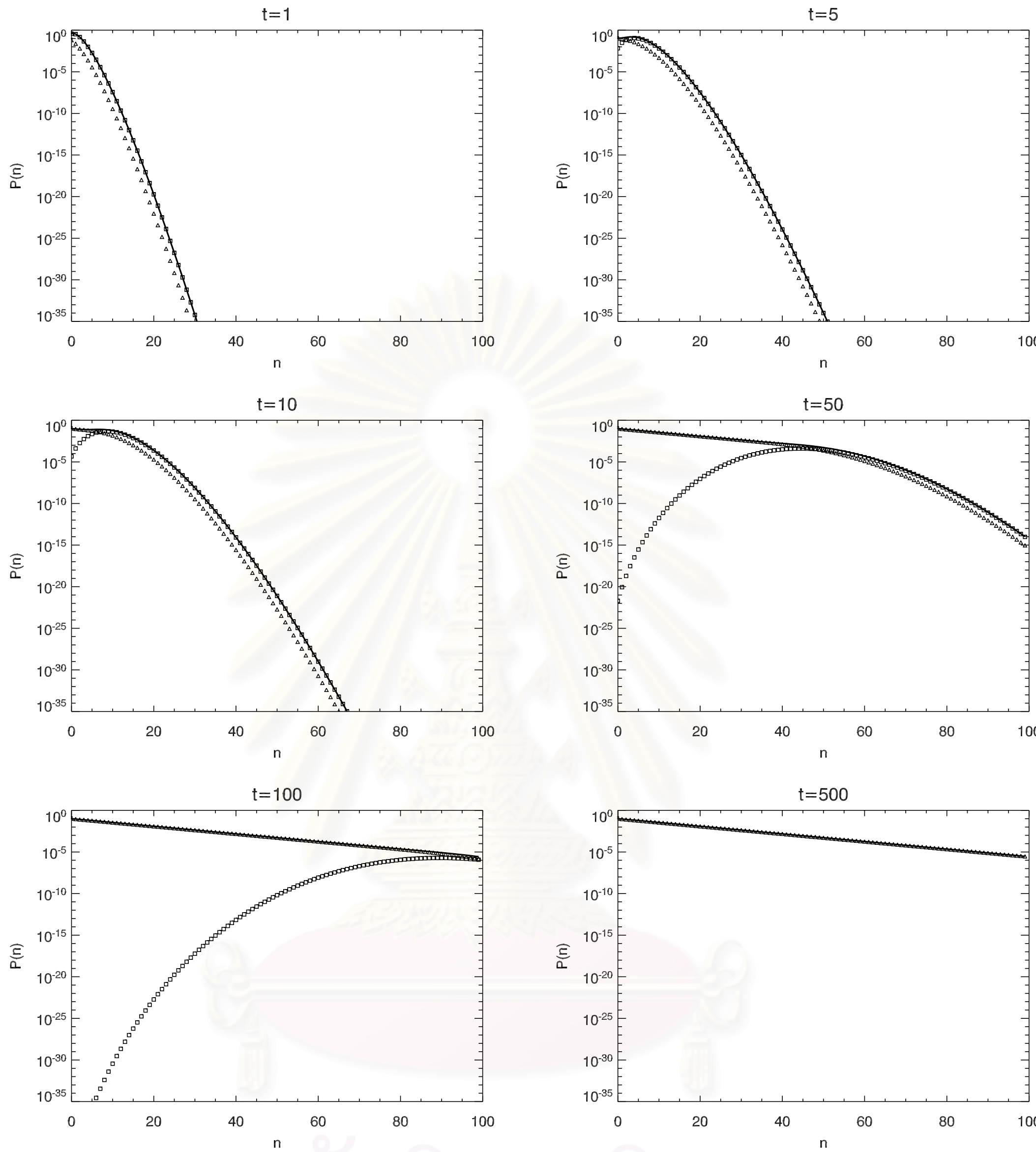


Figure 3.4: Analytic solution of $N(n,t)$ from equation (3.11) where $r$ = 0.9, $\epsilon$ = 0.1. Triangles: first term in (3.11). Squares: second term. Line: combined solution $N(n,t)$. At a very long time the solution approaches a power law, where $n$ is related to $\log p$.

• **Consider that $r$ and $\epsilon$ depend on the number of acceleration events**

In the real situation for IP shock acceleraton in ESP events, $r$ and $\epsilon$ are not constant because $r$ and $\epsilon$ depend on the particle velocity $v$.

When a particle moves across the shock, its velocity and momentum increase with the number of cycles $n$:

$$p_n = p_{n-1} + \frac{4}{3}\frac{(u_1 - u_2)}{v_{n-1}\cos\theta_1}p_{n-1}, \tag{3.12}$$

where $v_n$ is the velocity after the particle crosses back and forth across the shock $n$ times, and $p_n$ is the corresponding momentum ($v_n$ and $p_n$ are related to the kinetic energy $E_n$).

Following Drury (1983), but including the reflection probability for an oblique shock, we define the acceleration rate $r_n$ in terms of $v_n$ by

$$r_n = \Big[\frac{4}{v_n}\Big(\frac{\kappa_1 \sec\theta_1}{u_1} + [1 - \sqrt{1 - B_1/B_2}]\frac{\kappa_2 \sec\theta_2}{u_2}\Big)\Big]^{-1} \tag{3.13}$$

and we define the escape rate $\epsilon_n$ by

$$\epsilon_n = \left[\frac{4}{v_n}\Big(\frac{v_n\cos\theta_1}{4u_2}\Big(1+\frac{u_1}{v\cos\theta_1}\Big)^2 - 1\Big)\Big(\frac{\kappa_1\sec\theta_1}{u_1} + [1-\sqrt{1-B_1/B_2}]\frac{\kappa_2\sec\theta_2}{u_2}\Big)\right]^{-1}. \tag{3.14}$$

We get the partial diffential equation of $N(E,t)$ as

$$\frac{dN(E,t)}{dt} = I(E,t) - \epsilon_n(E,t)N(E,t) - \frac{\partial}{\partial E}[R(E,t)N(E,t)], \tag{3.15}$$

where $I$ is the inflow, $I(n,t) = I\delta_{n0}$, $R(E,t) = \Delta E/\Delta t$, and the initial condition is $N(n, t=0) = N_0$.

Considering the number of acceleration events at the shock, we can write a system of differential equations as

$$\frac{dN(n,t)}{dt} = I(t)\delta_{n0} - \epsilon_n N(n,t) - r_n N(n,t) + r_{n-1}N(n-1,t), \tag{3.16}$$

where we set $I(n,t) = I\delta_{n0}$.

The solution $N(n,t)$ in this case is

$$N(n,t) \;=\; I\,\epsilon_n \prod_{i=0}^{n-1} r_i \sum_{j=0}^{n} \frac{1-e^{-(r_j+\epsilon_j)t}}{(r_j+\epsilon_j)\prod_{\substack{k=0\\k\neq j}}^{n}(r_k-r_j+\epsilon_k-\epsilon_j)}$$
$$+N_0 \prod_{i=0}^{n-1} r_i \sum_{j=0}^{n} \frac{e^{-(r_j+\epsilon_j)t}}{\prod_{\substack{k=0\\k\neq j}}^{n}(r_k-r_j+\epsilon_k-\epsilon_j)}. \tag{3.17}$$

However, this result cannot be directly applied to our work because we do not want to make the assumption $I(n,t) = I\delta_{n0}$.

- **Derivation of cut-off in momentum and energy spectra**

From (3.3) and (3.4)

$$p_n \;=\; \Big(1+\frac{4}{3}\frac{(u_1-u_2)}{v_{n-1}\cos\theta_1}\Big)p_{n-1}$$
$$p_n \;=\; \Big(1+\frac{4}{3}\frac{(u_1-u_2)}{v_0\cos\theta_1}\Big)\Big(1+\frac{4}{3}\frac{(u_1-u_2)}{v_1\cos\theta_1}\Big)\cdots\Big(1+\frac{4}{3}\frac{(u_1-u_2)}{v_{n-1}\cos\theta_1}\Big)\;p_0,$$

where $v_0$ and $p_0$ are the initial velocity and momentum of particles, respectively.

We assume that $v_i$ is constant, with $v_i = v$ for all $i$. Thus

$$p_n \;\approx\; \Big[1+\frac{4}{3}\frac{(u_1-u_2)}{v\cos\theta_1}\Big]^n p_0$$
$$p_n \;\approx\; p_0 + n\frac{4}{3}m\frac{(u_1-u_2)}{\cos\theta_1}. \tag{3.18}$$

From the FTSA model (Ruffolo and Channok 2003; Channok et al. 2004), the rollover occurs at a number of acceleration events, $n$ (the number of times particles have crossed back and forth across the shock) that is related with time, $t$, and acceleration rate, $r$, by $n = rt$ (see Figure 3.4). We see that the cut-off momentum is

$$p_c \approx p_0 + \frac{4}{3} m \frac{(u_1 - u_2)}{\cos\theta_1} rt. \tag{3.19}$$

We use the acceleration rate, $r$ from (3.5) and (3.6), so

$$p_c \approx p_0 + \frac{4}{3} \frac{(u_1 - u_2)}{\cos\theta_1} \left[ \frac{mv/4}{\kappa_1 \sec\theta_1 / u_1 + (1 - \sqrt{1 - B_1/B_2}) \kappa_2 \sec\theta_2 / u_2} \right] t \tag{3.20}$$

Therefore the cut-off momentum increases with time.

Similarity, the cut-off velocity $v_c$ is

$$v_c \approx v_0 + \frac{(u_1 - u_2)}{3\cos\theta_1} \left[ \frac{1}{\kappa_1 \sec\theta_1 / u_1 + (1 - \sqrt{1 - B_1/B_2}) \kappa_2 \sec\theta_2 / u_2} \right] t \tag{3.21}$$

Considering the cut-off energy per nucleon $(E_c/A)$, $E_c/A \approx m_0 v_c^2/2$ (in the non-relativistic limit), we have

$$\frac{E_c}{A} \approx \frac{m_0}{2} \left\{ v_0 + \frac{(u_1 - u_2)}{3\cos\theta_1} \left[ \frac{1}{\kappa_1 \sec\theta_1 / u_1 + (1 - \sqrt{1 - B_1/B_2}) \kappa_2 \sec\theta_2 / u_2} \right] t \right\}^2 \tag{3.22}$$

where $A$ is the atomic mass number of the ion, and $m_0$ is the unified atomic mass unit. Therefore the cut-off energy $(E_c)$ increases with time squared $(t^2)$. After a very long time, the energy spectrum approaches a power law.

- **Including adiabatic deceleration**

Ruffolo (1995) and Ng, Reames and Tylka (1999) suggested that adiabatic deceleration may affect the acceleration time or acceleration rate, $r$. We consider momentum loss due to adiabatic deceleration assuming a nearly isotropic particle distribution

$$\langle \dot{p} \rangle = -\frac{2}{3} p \frac{V_{sw}}{R}, \tag{3.23}$$

where $V_{sw}$ is the solar wind speed, and $R$ is distance from the Sun.

The deceleration can be combined into $r_n$, the rate of acceleration events (rate of change of $n$), by using equation (3.18), so that

$$r_n = \left[\frac{4}{v_n}\left(\frac{\kappa_1 \sec\theta_1}{u_1} + [1-\sqrt{1-B_1/B_2}]\frac{\kappa_2 \sec\theta_2}{u_2}\right)\right]^{-1} - \frac{1}{2}\frac{v\cos\theta_1}{u_1-u_2}\frac{V_{sw}}{R}. \quad (3.24)$$

### 3.2.2 Numerical Model

The solution (3.17) is very complicated to use for calculating the distribution of particles in ESP events. Also, it fails to take into account the seed population. Therefore we construct a numerical model to simulate the implications of the FTSA model.

We use $E_n$ for the typical energy of a particle after it crosses the shock $n$ times. For example, we can write equation (3.15) as

$$\frac{dN(E_n,t)}{dt} = I(E_n,t) - (r_n + \epsilon_n)N(E_n,t) + r_{n-1}N(E_{n-1},t). \quad (3.25)$$

In the numerical model, we define $N(E_n, t=0) = N_0(E_n)$ as the initial condition for (3.25), where $N_0(E_n)$ is the upstream seed spectrum data from ULEIS observations. We define $I(E_n,t)$ as the inflow of particle flux (unit per time). We set $I(E_n,t) = \epsilon_n N_0(E_n)$.

In our numerical model we solve the system of ordinary differential equations (3.23) by the 4th order Runge-Kutta method (Press et al. 1992; Giordano 1997; Garcia 2000).

## 3.3 Calculation of Diffusion Coefficients in the FTSA Model

A key variable for calculating $r_n$ and $\epsilon_n$ in (3.13) and (3.14) is the diffusion coefficient, $\kappa$. We use the variable $\kappa_1$ (in the upstream region) and $\kappa_2$ (in the downstream region) as function of velocity ($v$) and particle mean free path ($\lambda$).

The diffusion coefficient is

$$\kappa = v\lambda/3,$$

where $\lambda$ is particle mean free path along the magnetic field (Forman 1975; Ellison, Baring and Jones 1995; Ruffolo 1999; Kallenrode 2001; Channok et al. 2004).

Decker and Vlahos (1986) and Jokipii (1987) proposed that in oblique shocks the rate of particle accceleration increases with the shock angle. Jokipii (1987) suggested that in the problem of diffusive shock acceleration, the diffusion coefficients are

$$\kappa_1 = v\frac{\lambda}{3}\cos^2\theta_1 \tag{3.26}$$

and

$$\kappa_2 = v\frac{\lambda}{3}\frac{\cos^2\theta_1}{(\cos^2\theta_1 + r^2\sin^2\theta_1)^{3/2}}, \tag{3.27}$$

where $r$ is the shock ratio, and $\lambda$ is particle mean free path along the magnetic field. From the relation between magnetic field strength and shock angle (from equation (3.1)) for a strong shock

$$\begin{aligned} B_1\cos\theta_1 &= B_2\cos\theta_2 \\ rB_1\sin\theta_1 &\approx B_2\sin\theta_2 \end{aligned}$$

so

$$rt_1 = t_2.$$

Then

$$\begin{aligned}\cos\theta_2 &= \frac{1}{\sec\theta_2} = \frac{1}{\sqrt{t_2^2+1}} = \frac{1}{\sqrt{r^2t_1^2+1}} = \frac{\cos\theta_1}{\sqrt{r^2\sin^2\theta_1+\cos^2\theta_1}} \\ \cos^3\theta_2 &= \frac{\cos^3\theta_1}{(r^2\sin^2\theta_1+\cos^2\theta_1)^{3/2}}.\end{aligned}$$

We therefore derive this limiting form of the Jokipii (1987) expression:

$$\kappa_2 = v\frac{\lambda}{3}\frac{\cos^3\theta_2}{\cos\theta_1}. \tag{3.28}$$

Clearly the particle mean free path $\lambda$ is a main factor determining the characteristics of spectra of energetic ions observed in ESP events.

Particle propagation in IP space from ESP events involves mean free paths over a wide range. The particle mean free path is different for each solar storm event. Mean free paths of ions in IP space may depend on the size of solar particle events (Reames 1989).

In the IP medium, the resonant scattering of energetic particles at Alfven waves plays an important role in particle propagation. Thus the particle mean free path is expected to depend only on particle's rigidity, $P$. A particle's rigidity is defined as its momentum per unit charge, $P = p/Q$, where $Q$ is its charge. For a power law, $\lambda \propto P^\alpha$ (Dröge 1994; Bieber et al. 1994; Kallenrode 2001; Sollitt 2004). Thus we write

$$\lambda = \lambda_0 P^\alpha \tag{3.29}$$

where $\alpha$ is a parameter that might vary for each solar event.

From many observations in the inner heliosphere, Forman (1981) suggested that $\lambda$ is about 0.01 AU in front of the shock wave and less than 0.0003 AU behind the shock wave. Ng, Reames and Tylka (1999) suggested that $\lambda$ is about $10^{-4}$ to $10^{-3}$ AU for ions at the shock wave.

Without any shocks, Palmer (1982) suggested that in IP space $\lambda$ is typically 0.08 to 0.3 AU. Beeck et al. (1987) suggested that $\lambda$ is about 0.05 to 0.1 AU. Mason et al. (1989) suggested that $\lambda$ is about 0.5 to 2 AU. Kallenrode, Wibberrenz and Hucke (1992) suggested that $\lambda$ is about 0.04 to 0.15 AU close to the Sun and $\lambda$ is about 0.04 to 0.3 AU at the orbit of the Earth.

# CHAPTER IV
# FTSA SIMULATIONS AND RESULTS

In this chapter we show simulations and results of the finite time shock acceleration (FTSA) model for the important interplanetary (IP) shock accelerated particles in the energetic storm particle (ESP) events.

## 4.1 FTSA Simulation

In simulations of the FTSA model, we calculate the results of the energy distribution function, $N(E)$, for solar energetic ions from IP shock acceleration and their energy spectra by a numerical method.

The procedure of the FTSA simulation model is performed in 7 steps:

**Step 1:** Select the ESP events. Identify the main parameters from *ACE* observations of the IP shock event (Desai et al. 2004) for use in the simulation:

$u_1$: upstream plasma fluid speed

$u_2$: downstream plasma fluid speed

$\theta_1$: upstream shock normal angle

$\theta_2$: downstream shock normal angle

$\rho_2/\rho_1$: density compression ratio

$B_2/B_1$: magnetic compression ratio

$A$: mass number of the ions

$Q$: charge number of the ions

$t$: time interval for an IP shock to propagate from the Sun to the *ACE* spacecraft.

Note that we consider $t$ from solar storm events. We use the time interval $t$ from the range of time from the CME occurrence at the Sun (from LASCO observations) to the time of shock passage at the *ACE* spacecraft following Cane and Richardson (2003).

**Step 2:** We set the minimum particle velocity $v_0$ (injection threshold) for acceleration by the IP shock, and the initial particle momentum $p_0$ for acceleration by the IP shock. Note that these are expressed in the upstream fluid frame.

**Step 3:** Calculate quantities for the particle acceleration process for the IP shock event from IP shock parameters in step 1.

We calculate the momentum $p_n$ and velocity $v_n$ that depend on $n$, the number of acceleration events of crossing the shock, from the following expressions:

$$\begin{aligned} p_1 &= p_0 + \frac{4}{3}\frac{(u_1 - u_2)}{v_0 \cos\theta_1} p_0 \\ p_2 &= p_1 + \frac{4}{3}\frac{(u_1 - u_2)}{v_1 \cos\theta_1} p_1 \\ &\vdots \\ p_n &= p_{n-1} + \frac{4}{3}\frac{(u_1 - u_2)}{v_{n-1} \cos\theta_1} p_{n-1} \end{aligned} \tag{4.1}$$

These could also simply be considered as grid values for discretizing the partial differential equation (3.25). After we get $p_n$ and $v_n$, next we

▶ calculate the kinetic energy of particles: $E_n$

$$E_n = \left( \frac{1}{\sqrt{1 - v_n^2/c^2}} - 1 \right) A m_0 c^2 \tag{4.2}$$

▶ calculate the particle rigidity: $P_n$

$$P_n = p_n c/Q \tag{4.3}$$

▶ calculate the particle's mean free path along the IP magnetic field: $\lambda_n$

$$\lambda_n = \lambda_0 (P_n/1\ \mathrm{MV})^\alpha \tag{4.4}$$

▶ calculate the diffusion coefficient upstream: $k_{1n}$

$$k_{1n} = v_n\ \frac{\lambda_n}{3}\cos^2\theta_1 \tag{4.5}$$

▶ calculate the diffusion coefficient downstream: $k_{2n}$

$$k_{2n} = v_n\ \frac{\lambda_n}{3}\frac{\cos^3\theta_2}{\cos\theta_1} \tag{4.6}$$

▶ calculate the acceleration rate: $r_n$

$$r_n = \Big[\frac{4}{v_n}\Big(\frac{k_{1n}\sec\theta_1}{u_1} + [1-\sqrt{1-B_1/B_2}]\frac{k_{2n}\sec\theta_2}{u_2}\Big)\Big]^{-1} \tag{4.7}$$

▶ calculate the escape rate: $\epsilon_n$

$$\begin{aligned}\epsilon_n \quad = \quad & \Bigg[\frac{4}{v_n}\Big(\frac{v_n\cos\theta_1}{4u_2}\Big(1+\frac{u_1}{v\cos\theta_1}\Big)^2 \ -1\Big) \\ & \times\Big(\frac{k_{1n}\sec\theta_1}{u_1} + [1-\sqrt{1-B_1/B_2}]\frac{k_{2n}\sec\theta_2}{u_2}\Big)\Bigg]^{-1}\end{aligned} \tag{4.8}$$

**Step 4:** Consider data from the observed upstream seed spectrum for the IP shock event. We set $N_0(E) = N_{\mathrm{seed}}(E)$ and define

$N(E_n, t=0) = N_0(E_n)$ as the initial condition for FTSA simulation,

$I(E_n) = \epsilon_n N_0(E_n)$ as the inflow function of seed particles.

**Step 5:** Use a numerical method to solve the numerical model of the system of ordinary differential equations from equation (3.25)

$$\frac{dN(E_n,t)}{dt} = I(E_n) - (r_n+\epsilon_n)N(E_n,t) + r_{n-1}N(E_{n-1},t) \tag{4.9}$$

by the fourth-order Runge-Kutta method (Press et al. 1998; 1992, Giordano 1997, Garcia 2000).

**Step 6:** Compare the simulation results with the observational data of IP shock accelerated spectra from ACE/ULEIS measurements (Desai et al. 2004).

**Step 7:** Consider whether these parameters of the particle mean free path ($\lambda = \lambda_0(P/\mathrm{MV})^{\alpha}$) provide the best fit to the data from the IP shock event. If the simulation results are not optimal, repeat steps 3, 4, 5, and 6.

## 4.2 Primary Results of FTSA Simulations

First we consider the interplanetary shock event on June 26, 1999 (Event#13 from Desai et al. 2003; 2004) to illustrate the effects of parameters in the FTSA simulation model such as minimum injection velocity of particles in the IP shock event, power index of particle rigidity, and time for the IP traveling shock events. Table 4.1 shows baseline parameters for iron ions for the IP shock event on June 24, 1999.

The observed seed spectrum of Fe is described by the function

$$N_0(E) = 0.0029E^{-1.373}\exp(-E/1.064). \tag{4.10}$$

where the function $N_0$ is the particle density, in units of particles/(cm$^2$ s sr MeV/nucleon), and $E$ is the kinetic energy per nucleon, in units of MeV/nucleon.

The sources of these values are indicated in Section 4.3. For now, we simply use them as baseline values for exploring the effects of each parameter.

The results of energy spectra from the FTSA simulations for Fe ions at various minimum particle velocities ($v_0$ = 200, 400, 600, and 800 km/s) are

Table 4.1 Baseline parameters for the event of June 24, 1999 with which to explore the influence of each parameter.

| parameters | symbol | value |
|---|---|---|
| plasma fluid speed upstream | $u_1$ | 131.0 km/s |
| plasma fluid speed downstream | $u_2$ | 56.4 km/s |
| shock normal angle upstream | $\theta_1$ | 50 deg |
| shock normal angle downstream | $\theta_2$ | 73 deg |
| density compression ratio | $\rho_2/\rho_1$ | 2.3 |
| magnetic compression ratio | $B_2/B_1$ | 2.2 |
| mass number of iron nuclei | $A_{Fe}$ | 56 |
| charge number of iron nuclei | $Q_{Fe}$ | 11.6 |
| mean free path of particles | $\lambda_0$ | 0.004 AU |
| power index of rigidity | $\alpha$ | 0.0 |
| initial velocity of particle | $v_0$ | 200 km/s |
| duration of ESP event | $t$ | 80 hours |

shown in Figure 4.1. We found that the minimum particle velocity ($v_0$) affects the energy spectra results only at low energy (see Figure 4.1). Observed seed spectra typically exhibit a power-law form at low energy (Desai et al. 2004), so seed particles are most abundant at the lowest momentum, $p_0$, corresponding to a suprathermal velocity of $v_0$ in the wind frame.

The results of energy spectra from the FTSA simulations for Fe ions at various power indices ($\alpha$) of particle rigidity by $\alpha$ = 0.0, 0.05, 0.10, 0.15, 0.20, 0.25, 0.30, and 0.35 are shown in Figure 4.2. We found that the power index ($\alpha$) of particle rigidity affects the energy spectra results (see Figure 4.2). Therefore we can adapt the value of $\alpha$ to achieve a good fit with observational data for various ions for each ESP events.

The results of energy spectra from the FTSA simulations for Fe ions at various times ($t$ = 20, 40, 80, 160, and 400 hours) are shown in Figure 4.3. From the simulation results (in Figure 4.3), we found that the FTSA model produces different characteristics of energy spectra at different times. We see that after a short time (20 hours) the particles receive only a small boost in energy. At intermediate times (40, 80, 160 hours), there is a power law at low energy and a rollover at a certain cut-off energy, $E_c$, followed by a drastic decline. We found that $E_c$ depends on time-squared ($t^2$) as in the theoretical model (see section 3.2.1). At a very long time (more than 400 hours), the spectrum approaches the classic steady-state power-law spectra over this energy range.

The results of energy spectra from the FTSA simulations for Fe ions at various shock normal angles upstream ($\theta_1$ = 15, 30, 45, and 60 degrees) are shown in Figure 4.4. We found that the shock normal angle affects the energy spectra characteristics (see Figure 4.4). There characteristics of shock structure and direction of IP magnetic field crossing the shock affect the shock accelerated particles in the IP medium, because the acceleration rate at the IP shock depends on the field-shock normal angle [see equations (3.4) and (3.5)].

The results of energy spectra from the FTSA simulations for Fe ions at various mean free paths ($\lambda_0$ = 0.004, 0.01, 0.04, and 0.1 AU) are shown in Figure 4.5. We found that the mean free path of particles ($\lambda_0$) affects the energy spectra characteristics (see Figure 4.5), by which a small mean free path can provide energy spectra at high energy that much have higher intensity than those for a large mean free path. In Figure 4.5 we see that $\lambda_0$ = 0.004 AU nearly fits the observed ESP Fe ion data. Therefore we can adapt the value of $\lambda_0$ that best fits the observed ESP data for each ESP event.

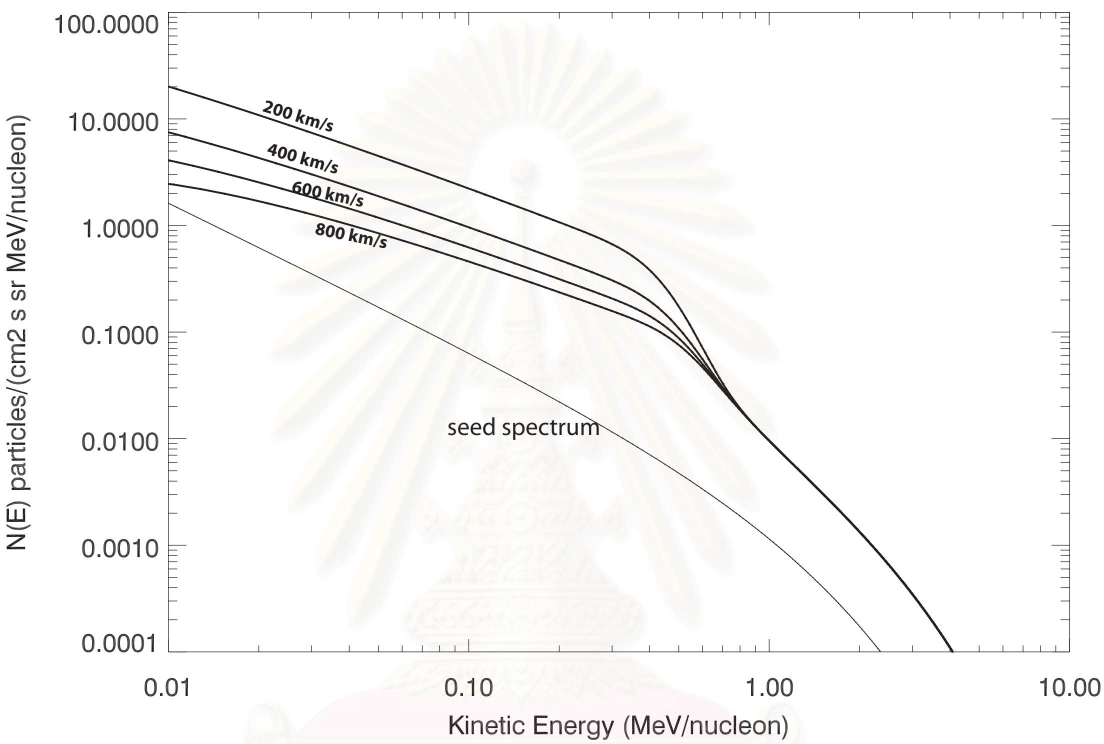


Figure 4.1: Energy spectra of Fe from FTSA simulations at various initial particle velocities, $v_0 = 200$, 400, 600, and 800 km/s.

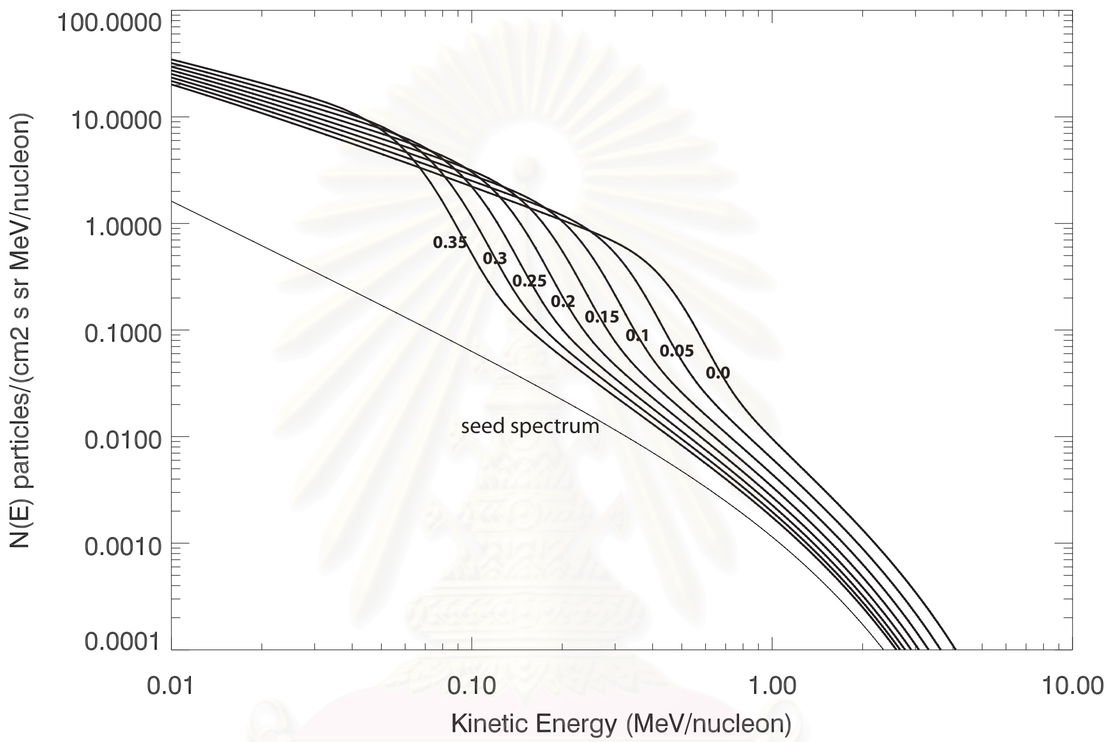


Figure 4.2: Energy spectra of Fe from FTSA simulations at various power indices of particle rigidity, $\alpha = 0.0$, 0.05, 0.10, 0.15, 0.20, 0.25, 0.30, and 0.35.

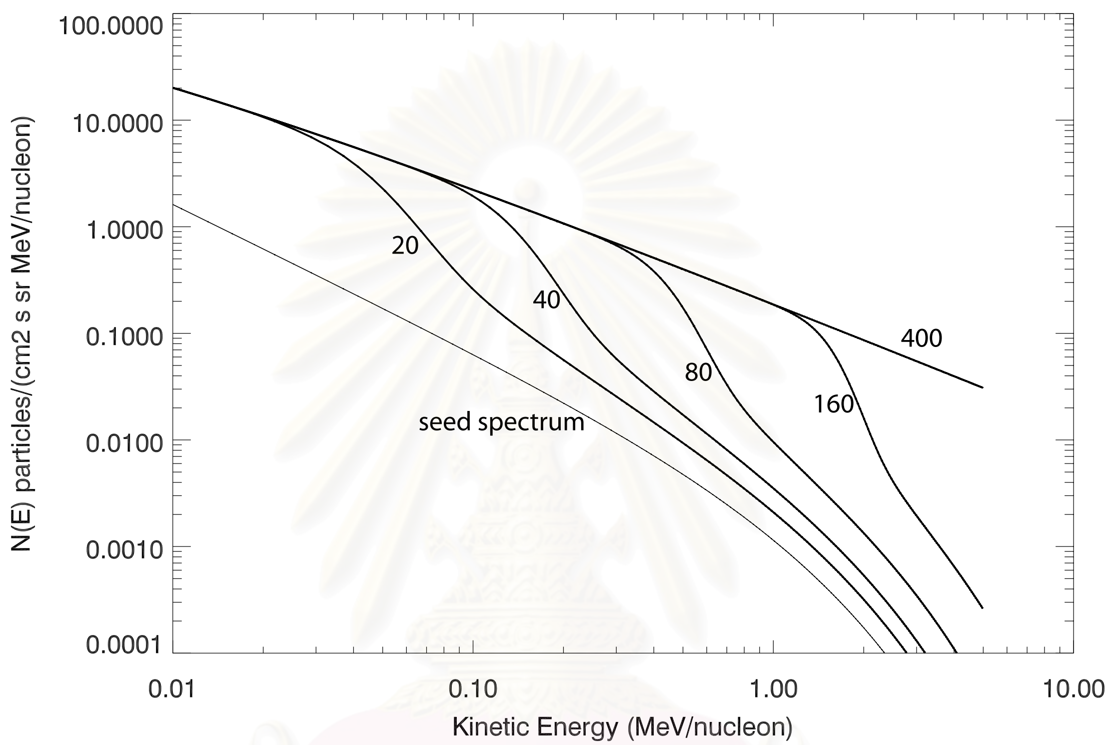


Figure 4.3: Energy spectra of Fe from FTSA simulations at different times, $t =$ 20, 40, 80, 160, 400 hours. After a very long time ($\geq$ 400 hours) energy spectra approach a power-law in this energy range.

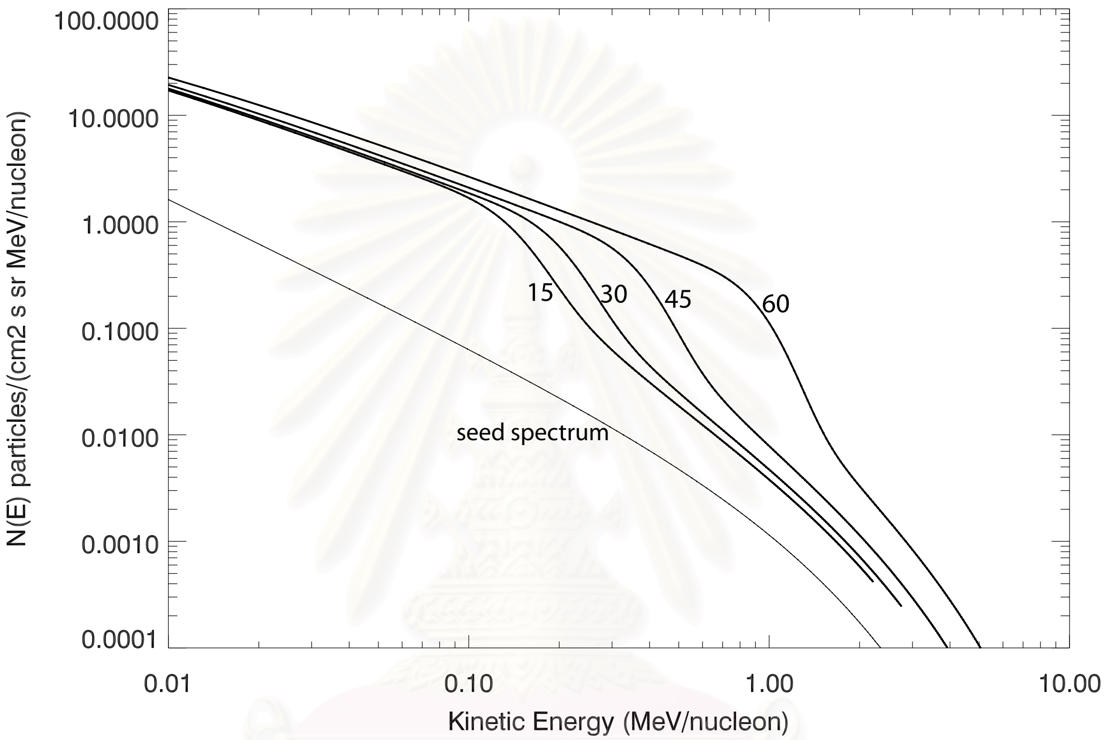


Figure 4.4: Energy spectra of Fe from FTSA simulations at various shock normal angles upstream, $\theta = 15$, 30, 45, and 60 degrees.

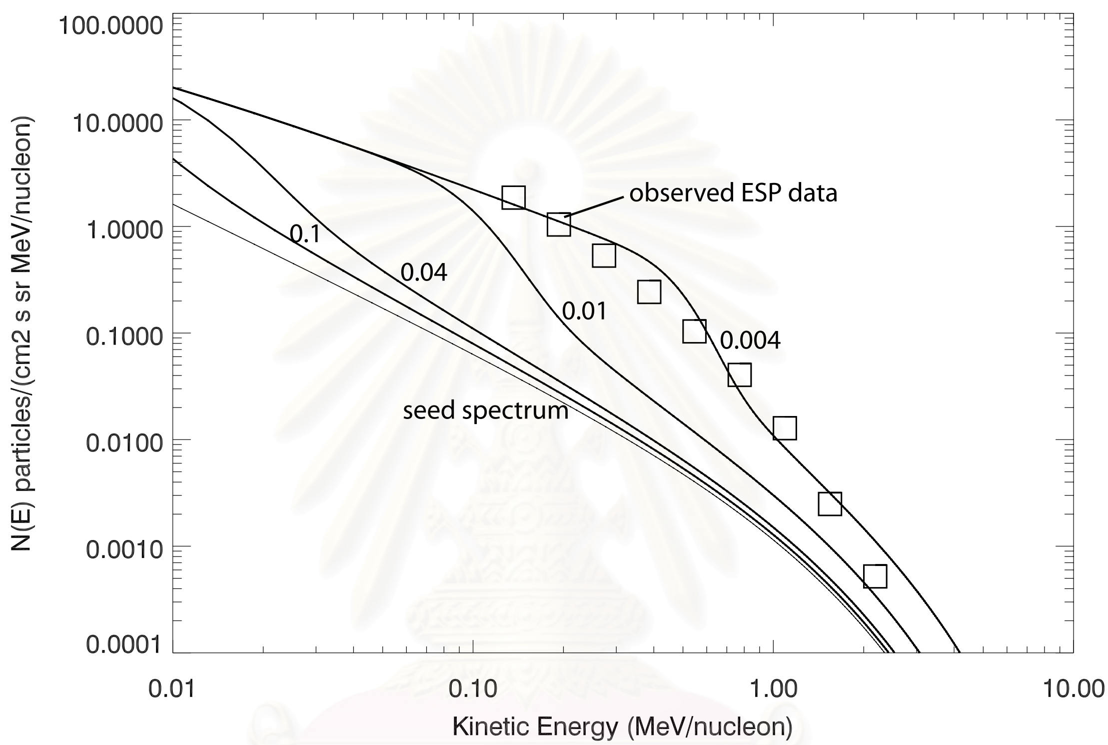


Figure 4.5: Energy spectra of Fe from FTSA simulations at various particle mean free paths, $\lambda_0 = 0.004$, 0.01, 0.04, and 0.1 AU.

## 4.3 Results for ESP Events

From primary results of FTSA simulations (Figures 4.1 – 4.5) we found that parameters $v_0$, $\lambda_0$, $\alpha$, $\theta$, and $t$ affect the IP shock spectra. In this section we show specific simulation results for 3 ESP events (Desai et al. 2003, 2004).

In our FTSA simulations, we use IP shock parameters and observed data for each ESP event from Desai et al. (2003), (2004). Some of the mean charge ($Q$) values are from Kleckler et al. (1999) and Möbius et al. (1999). We evaluate the duration $t$ for each ESP event from Cane and Richardson (2003) observations. We set the minimum particle velocity as $v_0$ = 200 km/s, which corresponds to a suprathermal velocity in the solar wind frame. We fit the 3 ESP events by optimizing $\lambda_0$ and $\alpha$ to provide the best fit with C, O, and Fe ion spectra for each event by minimizing the chi-squared

$$\chi^2 = \sum (\log N_{obs} - \log N_{sim})^2, \tag{4.11}$$

where $N_{obs}$ is the observed particle density from IP shock events (Desai et al. 2004) and $N_{sim}$ is the particle density from FTSA simulation.

### 4.3.1 Results for ESP Event on June 26, 1999

Parameters of this IP shock event (Event#13 from Desai et al. 2003; 2004) are in Table 4.2.

Table 4.2 Parameters for the IP shock event of June 24, 1999.

| Parameters from IP shock event (Desai et al. 2004) | | |
|---|---|---|
| plasma fluid speed upstream | $u_1$ | 131.0 km/s |
| plasma fluid speed downstream | $u_2$ | 56.4 km/s |
| shock normal angle upstream | $\theta_1$ | 50 deg |
| shock normal angle downstream | $\theta_2$ | 73 deg |
| density compression ratio | $\rho_2/\rho_1$ | 2.3 |
| magnetic compression ratio | $B_2/B_1$ | 2.2 |
| mass number of carbon nuclei | $A_C$ | 12 |
| mass number of oxygen nuclei | $A_O$ | 16 |
| mass number of iron nuclei | $A_{Fe}$ | 56 |
| charge number of carbon nuclei | $Q_C$ | 5.6 |
| charge number of oxygen nuclei | $Q_O$ | 6.8 |
| charge number of iron nuclei | $Q_{Fe}$ | 11.6 |
| Parameters from FTSA model | | |
| mean free path of particles | $\lambda_0$ | 0.003 AU |
| power index of rigidity | $\alpha$ | 0.05 |
| initial velocity of particle | $v_0$ | 200 km/s |
| duration of ESP event | $t$ | 54.8 hours |

Simulation results for C, O and Fe ions during this IP shock event are shown in Figure 4.6.

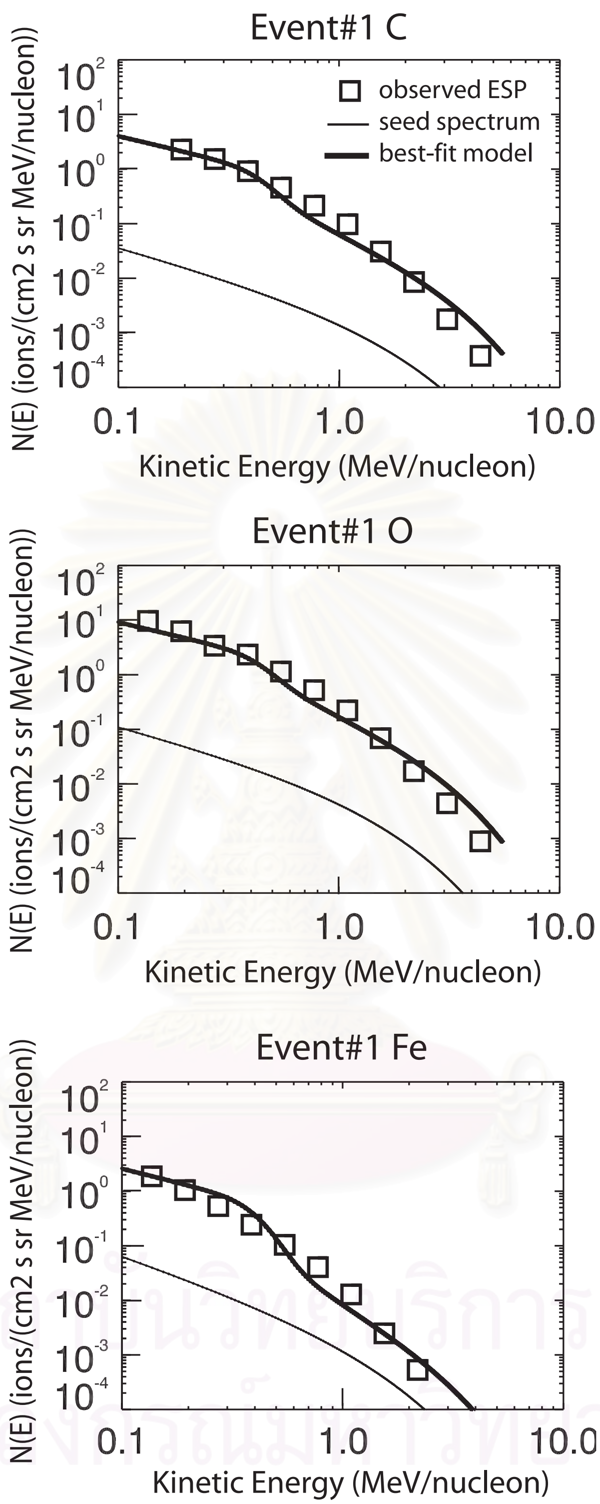


Figure 4.6: Simulation results and observations of spectra of C, O and Fe ions in the IP shock event on June 26, 1999.

### 4.3.2 Results for ESP Event on September 22, 1999

Parameters of this IP shock event (Event#18 from Desai et al. 2003; 2004) are in Table 4.3.

Table 4.3 Parameters for the IP shock event of September 22, 1999.

| Parameters from IP shock event (Desai et al. 2004) | | |
|---|---|---|
| plasma fluid speed upstream | $u_1$ | 131.0 km/s |
| plasma fluid speed downstream | $u_2$ | 54.6 km/s |
| shock normal angle upstream | $\theta_1$ | 64 deg |
| shock normal angle downstream | $\theta_2$ | 79 deg |
| density compression ratio | $\rho_2/\rho_1$ | 2.4 |
| magnetic compression ratio | $B_2/B_1$ | 2.3 |
| mass number of carbon nuclei | $A_C$ | 12 |
| mass number of oxygen nuclei | $A_O$ | 16 |
| mass number of iron nuclei | $A_{Fe}$ | 56 |
| charge number of carbon nuclei | $Q_C$ | 5.6 |
| charge number of oxygen nuclei | $Q_O$ | 6.8 |
| charge number of iron nuclei | $Q_{Fe}$ | 11.6 |
| Parameters from FTSA model | | |
| mean free path of particles | $\lambda_0$ | 0.039 AU |
| power index of rigidity | $\alpha$ | 0.08 |
| initial velocity of particle | $v_0$ | 200 km/s |
| duration time of ESP event | $t$ | 54.3 hours |

Simulation results for C, O and Fe ions during this IP shock event are shown in Figure 4.7.

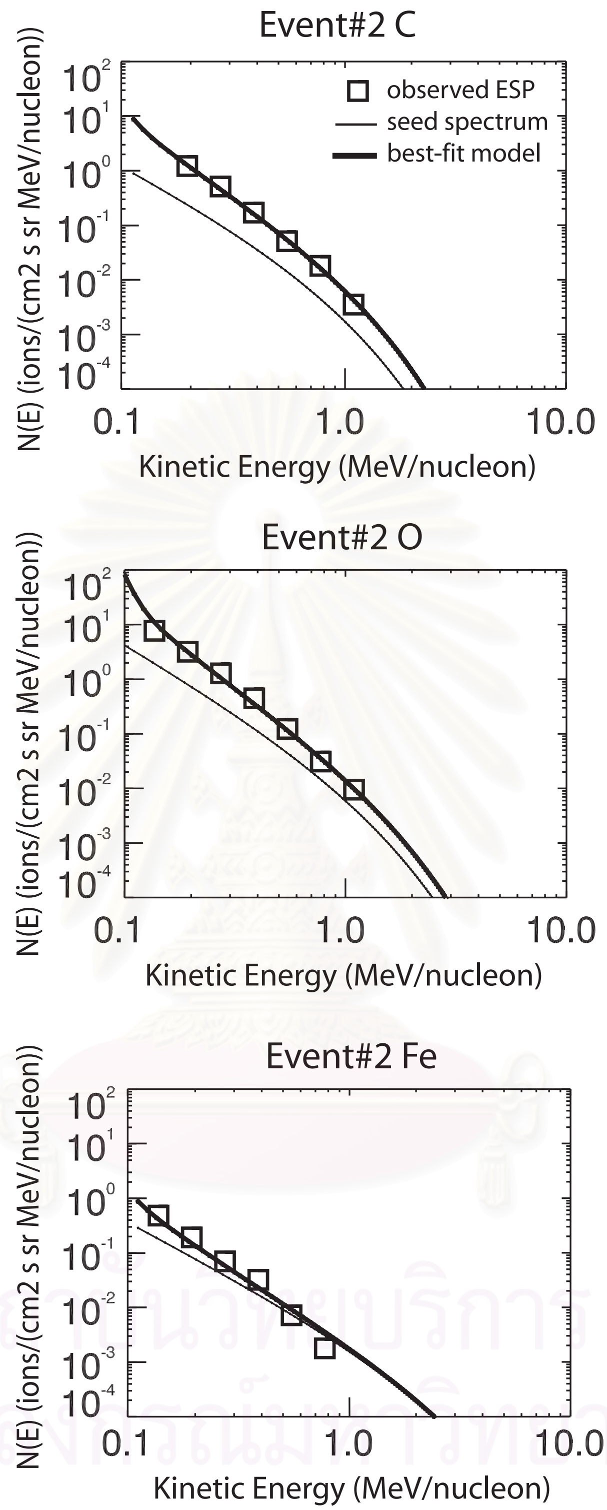


Figure 4.7: Simulation results and observations of spectra of C, O and Fe ions in the IP shock event on September 22, 1999.

### 4.3.3 Results for ESP Event on October 5, 2000

Parameters of this IP shock event (Event#37 from Desai et al. 2003; 2004) are in Table 4.4.

Table 4.4 Parameters for the IP shock event of October 5, 2000.

| Parameters from IP shock event (Desai et al. 2004) | | |
|---|---|---|
| plasma fluid speed upstream | $u_1$ | 188.0 km/s |
| plasma fluid speed downstream | $u_2$ | 78.3 km/s |
| shock normal angle upstream | $\theta_1$ | 66 deg |
| shock normal angle downstream | $\theta_2$ | 80 deg |
| density compression ratio | $\rho_2/\rho_1$ | 2.4 |
| magnetic compression ratio | $B_2/B_1$ | 2.3 |
| mass number of carbon nuclei | $A_C$ | 12 |
| mass number of oxygen nuclei | $A_O$ | 16 |
| mass number of iron nuclei | $A_{Fe}$ | 56 |
| charge number of carbon nuclei | $Q_C$ | 5.6 |
| charge number of oxygen nuclei | $Q_O$ | 6.8 |
| charge number of iron nuclei | $Q_{Fe}$ | 11.6 |
| Parameters from FTSA model | | |
| mean free path of particles | $\lambda_0$ | 0.10 AU |
| power index of rigidity | $\alpha$ | 0.08 |
| initial velocity of particle | $v_0$ | 200 km/s |
| duration time of ESP event | $t$ | 55.1 hours |

Simulation results for C, O and Fe ions during this IP shock event are shown in Figure 4.8.

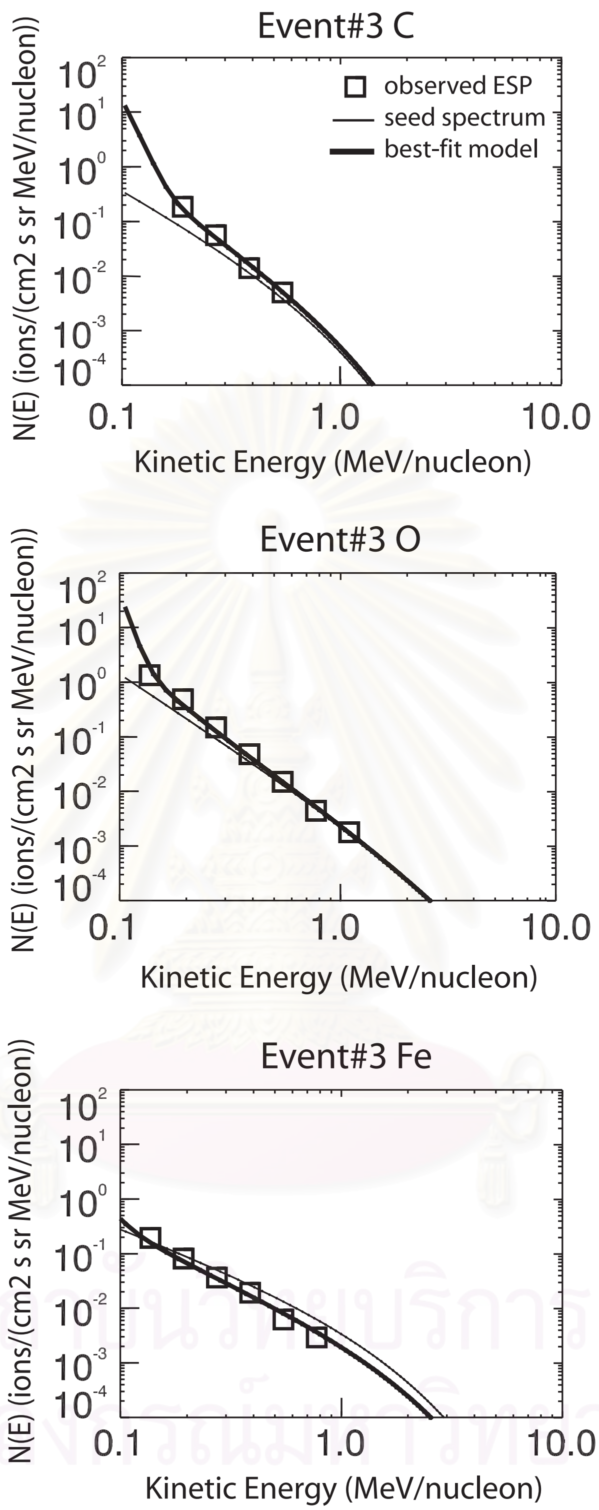


Figure 4.8: Simulation results and observations of spectra of C, O and Fe ions in the IP shock event on October 5, 2000.

## 4.4 Discussion

We have FTSA simulation and fitting results for three IP shock events on June 26, 1999, September 22, 2000, and October 5, 2000 (see Figures 4.6 – 4.8). We found that our FTSA model provides a good fit to observations of C, O, and Fe ions from ULEIS measurements (Desai et al. 2003; 2004) onboard the ACE spacecraft for all three events.

The mean free path ($\lambda$) of the energetic particles at the IP shock is very important for understanding more about particle scattering and propagation in the IP medium (Palmer 1982; Bieber et al. 1994; Dröge 1994; Zank, Rice, and Wu 2000; Kallenrode 2001; Khumlumlert 2001; Sollitt 2004).

In our FTSA simulations for determining mean free paths of the energetic particles, we consider the mean free path to follow a power law with particle rigidity, $\lambda = \lambda_0 (P/\mathrm{MV})^{\alpha}$ (Dröge 1994; Bieber et al. 1994; Kallenrode 2001; Sollit 2004). From FTSA simulation results, the optimal mean free paths of particles at the shock are different in the three IP shock events

- $\triangleright$ IP shock event on June 26, 1999: $\lambda = 0.003(P/\mathrm{MV})^{0.05}$ AU.
- $\triangleright$ IP shock event on September 22, 1999: $\lambda = 0.039(P/\mathrm{MV})^{0.08}$ AU
- $\triangleright$ IP shock event on October 5, 2000: $\lambda = 0.10(P/\mathrm{MV})^{0.08}$ AU

We see that in all three IP shock events the mean free path of particles is not constant but depends weakly on particle rigidity. In the IP shock event on June 26, 1999 we found that the mean free path of particles is smaller than for the other two IP shock events because the particle intensity of the IP shock event on June 26, 1999 is higher (see Appendix D). Thus a small mean free path implies high efficiency of acceleration, because the acceleration rate depends on $1/\kappa$ (Ruffolo and Channok 2003) where $\kappa$ is the diffusion coefficient. From the relation $\kappa \propto \lambda$, therefore a small particle mean free path improves the efficiency for acceleration to high energy.

The concept that a major CME-driven shock generates proton-amplified waves has been developed through a series of papers (e.g., Ng and Reames 1994; Ng et al. 1999, 2003) and yields an impressive explanation of unusual elemental ratios as a function of time on 1998 April 20 (Tylka et al. 1999) with $\lambda \sim 10^{-4}$ to $10^{-3}$ AU. Thus we might expect to find $\lambda$ values ranging from such low values, for strong events, to typical IP conditions with $\lambda_{||} \sim 0.08$ to 0.3 AU (Palmer 1982) for weaker events. Our fits to ion spectra of IP shock Event 1 (June 26, 1999) indeed yield a much lower $\lambda$ for this major ESP event, with $\lambda = 0.003$ AU at 1 MV. For Events 2 and 3 (September 22, 1999 and October 5, 2000), is similar to typical IP conditions. This confirms that proton-amplified waves are apparently significant for ion acceleration in major ESP events but not for weaker ESP events.

# CHAPTER V

# CONCLUSIONS

The finite-time shock acceleration (FTSA) model based on the diffusive shock acceleration mechanism (Bell 1978a; 1978b; Drury 1983; Ruffolo 1999) due to the finite time available for shock acceleration (see Klecker et al. 1981; Forman 1981; Lee 1983) was successful to quantitatively and qualitatively fit the energy spectra data of C, O,and Fe ions from important energetic storm particle (ESP) observations (June 26, 1999, September 22, 1999, and October 5, 2000; see Desai et al. 2003; 2004). The ESPs result from interplanetary (IP) shock acceleration of electrons and ions in the IP medium near the Earth (about 1 AU from the Sun).

In the FTSA model we refer to gradual solar events that have a large solar flare and coronal mass ejection (CME) in which solar energetic particles and other suprathermal particles are accelerated by CME-driven shocks in the IP medium beyond the outer corona of the Sun. We do not address particles accelerated at site of the flare at the solar surface, or by a CME-driven shock near the Sun.

The FTSA model can describe characteristics of an energetic seed particle population (seed spectrum) that is accelerated to higher energy (shock spectrum) by an IP shock passage due to a large solar flare event. Mason, Mazur, and Dwyer (1999) suggested that remnant flare material could be an important component of the seed population that is available for acceleration at IP shocks driven by CMEs. Thus IP shock should accelerate energetic ions provided that they encounter remnant flare material about 1 AU.

For each IP shock event the characteristic shock properties are not the same, and times for IP shock propagation in IP space are different. Therefore we see that observed data from IP shock events are different for each event. Therefore the FTSA model is a good way to study the effect of particle acceleration from IP shocks and energy spectra of accelerated particles in terms of the finite time of the ESP events or the solar storm events.

Many recent research works (e.g., Tylka 2001; Klecker et al. 2003; Desai et al. 2003; 2004) used the empirical formula of Ellison and Ramaty (1985) to fit the characteristics of energetic particle shock spectra with the rollover energy, $E_c$:

$$N(E) = N_0 E^{-\gamma} \exp(-E/E_c). \tag{5.1}$$

Ellison and Ramaty (1985) suggested that $E_c$ depends on the particle diffusion length or size of the shock (Ellison 1984; Ellison and Ramaty 1985) by $\kappa/u$ where $\kappa$ is the diffusion coefficient and $u$ is shock speed relative to the upstream fluid. Anyway, the Ellison and Ramaty (1985) formula cannot completely fit spectra of the ESP events (such as the ESP event on October 5, 2000; from Desai et al. 2004). In the October 5, 2000 ESP event, Desai et al. (2004) fit the energetic ion spectra with the Ellison and Ramaty (1985) formula (equation 5.1) for C, O, and Fe to obtain

$$N_C(E) \;=\; 0.000527E^{-3.575}$$

$$N_O(E) = 0.002229E^{-3.248}$$
$$N_{Fe}(E) = 0.001724E^{-2.375}.$$

In results from Desai et al. (2004) fitting observed ESP data there is no exponential term because $E_c$ (in 5.1) is very large, but the value of $\kappa/u$ in this event is not very large. Even at an energy as low as 3 keV/nucleon, $\kappa/u \sim 1 \times 10^{10}$ km, whereas the shock width is $\sim 6 \times 10^6$ km. Therefore, the criterion $\kappa/u \sim$ (shock width) would imply a very low rollover energy. Therefore the fit of Ellison and Ramaty (1985) formula with $E_c$ as the energy where $\kappa/u \sim$ (shock width) in the October 5, 2000 ESP event is not good. Our FTSA model can provide a good fit simultaneously to C, O, and Fe ESP spectra from observed data in the October 5, 2000 event (see Section 4.3). We think the rollover energy from the $\kappa/u$ effect cannot provide a good explanation of the IP shock acceleration in ESP events.

## Summary of conclusions of the FTSA model for IP shock acceleration

- The FTSA model can explain rollovers at energies of about 0.1 - 10 MeV/nucleon (Desai et al. 2003; 2004) in terms of the finite time available for shock acceleration. This time, $t$, corresponds to observed data from ULEIS measurements on the *ACE* spacecraft near the Earth. Near the Earth, the acceleration time is typical on the order of $t$, or about 3 - 5 days, and the observed spectrum rolls over due to the finite time.

- The FTSA model provides a good explanation of observed changes in energetic ion (C, O, Fe) spectra from IP shock events. It can explain the puzzling results that the high energy ion (C, O, Fe) spectra sometimes steepen after IP shock passage.

• The fully developed FTSA model can explain characteristics of ion spectra in ESP events better than Ruffolo and Channok (2003) or Channok et al. (2004). The results of Ruffolo and Channok(2003) and Channok et al. (2004) had a problem about a hump component in the spectra of energetic ions, because they did not consider the flowing effect of particles in the IP medium.

• The FTSA model can explain characteristics of the rollover energy, $E_c$, in ESP events better than Ellison and Ramaty (1985), who used an empirical formula (equation 5.1) to fit energy spectra of electrons and ions in solar flare events.

• In the FTSA model, the particle mean free path, $\lambda$ can depend on rigidity, $P$, with the power index, $\alpha$, so that $\lambda \propto P^{\alpha}$. We find very low values of $\alpha$, so in fact that dependence is very weak. We derive a cut-off rigidity, $P_c$ from Ruffolo and Channok (2003),

$$P_c = \left[P_0^{\alpha+1} + \frac{4}{3}(\alpha+1)\frac{A}{Q}\frac{m_0 c}{e}\frac{u_1 - u_2}{\cos\theta_1} r_0 P_0^{\alpha} t\right]^{1/(\alpha+1)}, \tag{5.2}$$

where $P_0$ is the initial particle rigidity, $r_0$ is the initial acceleration rate, $A$ is the mass number of the ions, $Q$ is the charge number of the ions, and $t$ is the acceleration time. Thus the cut-off energy per nucleon is

$$E_c/A \propto (Q/A)^{2\alpha/(\alpha+1)} t^{2/(\alpha+1)}. \tag{5.3}$$

Therefore the cut-off energy per nucleon ($E_c/A$) depends on the effect of the acceleration time scale (Lee 1983; Lee and Ryan 1986; Zank, Rice, and Wu 2000) and charge per nucleon, $Q/A$ (e.g., Tylka 2001; Reames and Tylka 2002; Klecker et al. 2003).

From ULEIS observations of IP shock events, Desai et al. (2003, 2004) found that $E_c$ of C, O, and Fe ions does not depend on the charge per nucleon

$(Q/A)$ for all 72 events, whereas the FTSA theory can describe the characteristic of $E_c$ in IP shock events in terms of the finite time.

# REFERENCES


Abraham-Shrauner, B. 1972. Determination of magnetohydrodynamic shock normal. *Journal of Geophysical Research* 77: 736–739.

Achterberg, A. 1988. Shock acceleration in disordered magnetic field. *Monthly Notices of Royal Astronomical Society* 232: 323–337.

Aschwanden, M.J. 2004. *Physics of the Solar Corona.* Chichester UK: Praxis Publishing.

Axford, W.I. 1981a. Acceleration of cosmic rays by shock waves. *Proceedings of the 17th International Cosmic Ray Conference* 12: 155–203. Paris France: Centre d' Etudes de Saclay.

Axford, W.I. 1981b. The acceleration of cosmic rays by shock waves. *Annals of the New York Academy of Sciences* 375: 297–313.

Axford, W.I., Leer, E., and Skadron, G. 1977. The acceleration of cosmic rays by shock waves. *Proceedings of the 15th International Cosmic Ray Conference* 11: 132–137. Budapest, Hungary: Institute for Nuclear Research and Nuclear Energy.

Baring, M.G., Ogilvie, K.W., Ellison, D.C., and Forsyth, R.J. 1997. Acceleration of solar wind ions by nearby interplanetary shocks: Comparison of Monte Carlo simulations with ULYSSES observations. *Astrophysical Journal* 476: 889–902.

Bell, A.R. 1978a. The acceleration of cosmic rays in shock fronts–I. *Monthly Notices of Royal Astronomical Society* 182: 147–156.

Bell, A.R. 1978b. The acceleration of cosmic rays in shock fronts–II. *Monthly Notices Royal of Astronomical Society* 182: 433–455.

Bieber, J.W, Matthaeus, W.H., Smith, C.W., Wanner, W., Kallenrode, M.-B., and Wibberenz, G. 1994. Protons and electron mean free paths: The Palmer consensus range revisited. *Astrophysical Journal* 420: 294–306.

Blandford, R.D., and Ostriker, J.P. 1978. Particle acceleration by astrophysical shocks. *Astrophysical Journal* 221: L29–L32.

Bryant, D.A., Cline, U.D., Desai, U.D., and McDonald, F.B. 1962. Explorer 12 observation of solar cosmic rays and energetic storm particles after solar flare of September 28, 1961. *Journal of Geophysical Research* 67: 4953–4961.

Burlaga, L.F. 1995. *Interplanetary Magnetohydrodynamics.* New York: Oxford University Press.

Campbell, W.H. 2001. *Earth Magnetism*. Massachusetts: Harcourt/Academic Press.

Cane, H.V. 1995. The structure and evolution of interplanetary shocks and the relevance for particle acceleration. *Nuclear Physics B Proceedings Supplements* 39A: 35–44.

Cane, H.V., McGuire, R.E., and von Rosenvinge, T.T. 1986. Two classes of solar energetic particle events associated with impulsive and long-duration soft X-ray flares. *Astrophysical Journal* 301: 448–459.

Cane, H.V., and Richardson, I.G. 2003. Interplanetary coronal mass ejections in the near-Earth solar wind during 1996–2002. *Journal of Geophysical Research* 108: 1156–1172.

Caso, C. et al. 1998. Review of particle physics. *The European Physical Journal C* 3: 1–794.

Channok, C., Ruffolo, D., Desai, M., and Mason, G. 2004. Finite time shock acceleration at interplanetary shocks. *Proceedings of the 8th Annual National Symposium on Computational Science and Engineering* 107–110. Nakorn Ratchasima: Suranaree University of Technology.

Christian, E.R., Jacob, S.B., Margolies D.L., Mewaldt R.A., and Ormes J.E. 1997. *Advanced Composition Explorer*. Washington DC: NASA.

Clem, J.M., and Dorman L.I. 2000. Neutron monitor response functions. *Space Science Reviews* 93: 335–359.

Cliver, E.W. 2000. Solar energetic particles: Acceleration and transport. in Dingus, B.L., Kieda, D.B., and Salamon, M.H. (ed.), *AIP Conference Proceedings Vol. 516: 26th International Cosmic Ray Conference*, pp.103–119. New York: AIP Press.

Colburn, D.S. and Sonett, C.P. 1966. Discontinuities in the solar wind. *Space Science Reviews* 5: 439–459.

Cravens, T.E. 1997. *Physics of Solar System Plasmas*. New York: Cambridge University Press.

Decker, R.B., Pesses, M.E., and Krimigis, S.M. 1981. Shock associated low-energy ion enhancements observed by Voyager 1 and 2. *Journal of Geophysical Research* 86: 8819–8831.

Decker, R.B., and Vlahos, L. 1986. Numerical studies of particle acceleration at turbulent, oblique shocks with an application to prompt ion acceleration during solar flares. *Astrophysical Journal* 306: 710–729.

de Hoffmann, F., and Teller, E. 1950. Magneto-Hydrodynamic Shocks. *Physical Review* 80: 692–703.

Desai, M.I., Mason, G.M., Dwyer, J.R., Mazur, J.E., Gold, R.E., Krimigis, S.M., Smith, C.W., and Skoug, R.M. 2003. Evidence for a suprathermal seed population of heavy ions accelerated by interplanetary shocks near 1 AU. *Astrophysical Journal* 588: 1149–1162.

Desai, M.I., Mason, G.M., Dwyer, J.R., Mazur, J.E., Smith, C.W., and Skoug, R.M. 2001. Acceleration of 3He nuclei at interplanetary shock. *Astrophysical Journal* 553: L89–L92.

Desai, M.I., Mason, G.M., Wiedenbeck, M.E, Cohen, C.M., Mazur. J.E., Dwyer, J.R., Gold, R.E., Krimigis, S.M., Hu, Q., Smith, C.W., and Skoug, R.M. 2004. Spectral properties of heavy ions associated with the passage of interplanetary shocks at 1 AU. *Astrophysical Journal* 611: 1156–1174.

Dröge, W. 1994. Transport of solar energetic particles. *Astrophysical Journal Supplement* 90: 567–576.

Drury, L.O'C. 1983. An introduction to the theory of diffusive shock acceleration of energetic particles in tenuous plasmas. *Reports on Progress in Physics* 46: 973–1027.

Ellison, D. 1984. Shock acceleration of diffuse ions at the Earth's bow shock: Acceleration efficiency and A/Z enhancement. *Journal of Geophysical Research* 90: 29–38.

Ellison, D., Baring, M., and Jones, F. 1995. Acceleration Rates and Injection Efficiencies in Oblique Shocks. *Astrophysical Journal* 453: 873–882.

Ellison, D., and Ramaty, R. 1985. Shock acceleration of electrons and ions in solar flares. *Astrophysical Journal* 298: 400–408.

Fermi, E. 1949. On the origin of the cosmic ray radiation. *Physical Review* 5: 1169–1174.

Fermi, E. 1954. Galactic magnetic fields and the origin of cosmic ray radiation. *Astrophysical Journal* 119: 1–6.

Forbush, S.E. 1946. Three unusual cosmic ray increases possibly due to charged particles from the Sun. *Physical Review* 70: 711–772.

Forman, M.A. 1981. Acceleration theory for 5-40 keV ions at interplanetary shock. *Advances in Space Research* 1: 97–100.

Forman, M.A. and Morfill, G. 1979. Time-dependent acceleration of solar wind plasma to MeV energies at co-rotating interplanetary shocks. *Proceedings of the 16th International Cosmic Ray Conference* 5: 328–332. Kyoto, Japan: Universal Academy Press.

Foukal, P. 1990. *Solar Astrophysics.* New York: John Wiley & Sons.

Garcia, A.L. 2000. *Numerical Methods for Physics.* 2nd ed. New Jersey: Prentice Hall.

Giordano, N.J. 1997. *Computational Physics.* New Jersey: Prentice Hall.

Gloeckler, G., Schwadron, N.A., Fisk, L.A., and Geiss, J. 1995. Weak pitch angle scattering of few MV rigidity ions from measurements of anisotropies in the distribution function of interstellar pickup H+. *Geophysical Research Letters* 22: 2665–2668.

Gopalswamy, N., Yashiro, S., Stenborg, G., and Howard, R. 2003. Coronal and interplanetary environment of large solar energetic particle events. *Proceedings of the 28th International Cosmic Ray Conference* 6: 3549–3552. Tokyo, Japan: Universal Academy Press.

Gosling, J.T., Asbridge, J.R., Bame, S.J., Feldman, W.C., Zwickl, R.D., Paschmann, G, Sckopke, N., and Hynds, R.J. 1981. Interplanetary ions during an energetic storm particle event: The distribution function from solar wind thermal energies to 1.6 MeV. *Journal of Geophysical Research* 86: 547–554.

Groom, D.E. et al. 2000. Review of particle physics. *The European Physical Journal C* 15: 1-878.

Ho, G.C., Lario, D., Decker, R.B., Roelof, E.C., Desai, M., and Smith, C.W. 2003. Energetic electrons associated with transient interplanetary shocks: Evidence for weak interaction. *Proceedings of the 28th International Cosmic Ray Conference* 6: 3689–3692. Tokyo, Japan: Universal Academy Press.

Jokipii, J.R. 1966. Cosmic-ray propagation I. Charged particles in a random magnetic field. *Astrophysical Journal* 146: 480–487.

Jokipii, J.R. 1987. Rate of energy gain and maximum energy in diffusive shock acceleration. *Astrophysical Journal* 313: 842–846.

Jones, F.C., and Ellison, D.C. 1991. The plasma physics of shock acceleration. *Space Science Reviews* 58: 259–346.

Kallenrode, M.-B. 2001. *Space Physics: An Introduction to Plasmas and Particles in the Heliosphere and Magnetosphere.* Heidelberg: Spinger-Verlag.

Kallenrode, M.-B., Cliver, E.W, and Wibberenz, G. 1992. Composition and azimuthal spread of solar energetic particles from impulsive and gradual flare. *Astrophysical Journal* 391: 370–379.

Kallenrode, M.-B., Wibberenz, G., and Hucke, S. 1992. Propagation conditions of relativistic electrons in the inner heliosphere. *Astrophysical Journal* 394: 351–356.

Khumlumlert, T. 2001. *Injection Function of Energetic Heavy Ions from the Sun.* Ph.D. Thesis. Department of Physics, Faculty of Science, Chulalongkorn University.

Kirk, J.G. 1988. Pitch-angle anisotropy of low-energy ions at interplanetary shocks. *Astrophysical Journal* 324: 557–565.

Kirk, J.G. 1994. Particle acceleration. In Benz, A.O. and Couvoisier, T.L.-L. (ed.), *Plasma Astrophysics*, 225–314. Heidenberg: Springer-Verlag.

Kirk, J.G., and Dendy, R.O. 2001. Shock acceleration of cosmic rays: A critical review. *Journal of Physics G: Nuclear and Particle Physics* 27: 1589–1595.

Klecker, B.M., Möbius, E., Popecki, M.A., Kistler, L.M., Bogdanov, A., Galvin, A.B., Heirtzler, D., Morris, D., Hovestadt, D. 1999. The ionic charge composition of CME related solar energetic particles events as observed with SEPICA onboard ACE. *Proceedings of the 26th International Cosmic Ray Conference* 6: 83–86.

Klecker, B.M., Popecki, M.A., Mobius, E., Desai, I.M, Mason, G.M., and Wimmer-Schweingruber R.F. 2003. On the energy dependence of ionic charge states. *Proceedings of the 28th International Cosmic Ray Conference* 6: 3277–3280. Tokyo, Japan: Universal Academy Press.

Klecker, B.M., Scholer, D., Hovestaldt, G., Gloeckler G., and Ipavich F.M. 1981. Spectral and compositional variations of low energy ions during an energetic storm particles event. *Astrophysical Journal* 251: 393–401.

Krymskii, G.F. 1977. A regular mechanism for the acceleration of changed particles on the front of a shock wave. *Soviet Physics Doklady* 22: 327–328.

Kocharov, L., and Torsti, J. 2003. The origin of high-energy $^3$He-rich solar particle events. *Astrophysical Journal* 586: 1430–1435.

Lagage, P.O., and Cesarsky, C.J. 1983a. Cosmic-ray shock acceleration in the presence of self-excited waves. *Astronomy and Astrophysics* 118: 223–228.

Lagage, P.O., and Cesarsky, C.J. 1983b. The maximum energy of cosmic rays accelerated by supernova shocks. *Astronomy and Astrophysics* 125: 249–257.

Lang, K.R. 2000. *The Sun from the Space.* Heidelberg: Springer-Verlag.

Lang, K.R. 2001. *The Cambridge Encyclopedia of the Sun.* Cambridge UK: Cambridge University Press.

Lee, M.A. 1983. Coupled hydromagnetic wave excitation and ion acceleration at interplanetary traveling shocks. *Journal of Geophysical Research* 88: 6109–6119.

Lee, M.A. 2000. Acceleration of energetic particles on the Sun, in the heliosphere, and in the galaxy, in Mewaldt, R.A., Jokipii, J.R., Lee, M.A., Möbius, E., and Zurbuchen, T.H. (ed.), *AIP Conference Proceedings Vol. 528: Acceleration and Transport of Enegetic Particles Observed in Heliosphere* pp.3–18. New York: AIP Press.

Lee, M.A., and Ryan, J.M. 1986. Time-dependent coronal shock acceleration of energetic solar flare particles. *Astrophysical Journal* 303: 892–842.

Leerungnavarat, K. 2004. *Modeling of Forbush Decreases in Cosmic Rays.* Ph.D. Thesis. Department of Physics, Faculty of Science, Chulalongkorn University.

Lin, R.P. 2004. New RHESSI results on particle acceleration and energy release in solar flares. *Proceedings of the 28th International Cosmic Ray Conference* 8: 335–340. Tokyo, Japan: Universal Academy Press.

Lockwood, J.A., Webber, W.R., and Hsieh, L. 1974. Solar flare proton rigidity spectra deduced from cosmic ray neutron monitor observations. *Journal of Geophysical Research* 79: 4149–4155.

Longair, M.S. 1992. *High Energy Astrophysics Vol.1.* 2nd ed. Cambridge: Cambridge University Press.

Longair, M.S. 1994. *High Energy Astrophysics Vol.2.* 2nd ed. Cambridge: Cambridge University Press.

Manchester, W.B.,IV, Gombosi, T.I., De Zeeuw, D.L., Sokolov, I.V., Roussev, I.I., Powell, K.G., Kóta, J., Tóth, G., and Zurbuchen, T.H. 2005. Coronal mass ejection shock and sheath structures relevant to particle acceleration. *Astrophysical Journal* 622: 1225–1239.

Mason, G.M., Gloeckler, G., and Hovestadt, D. 1984. Temporal variations of nucleonic abundances in solar flare energetic particle events. II - Evidence for large-scale shock acceleration. *Astrophysical Journal* 280: 902–916.

Mason, G.M., Gold, R.E., Krimigis, S.M., Mazur, J.E., Andrews, G.B., Daley,K.A., Dwyer,J.R., Heuerman, K.F., James, T.L., Kennedy, M.J., Lefevere, T., Malcolm,H., Tossman, B., and Walpole, P.H. 1998, The Ultra-Low-Energy Isotope Spectrometer (ULEIS) for the ACE spacecraft. *Space Science Reviews* 86: 409–448.

Mason, G.M., Mazur, J.E., and Dwyer, J.R. 1999. $^3$He enhancements in large solar energetic particle events. *Astrophysical Journal* 525: L133–L136.

Mason, G.M., Ng, C.K., Klecker, B., and Green, G. 1989. Impulsive acceleration and scatter-free transport of about 1 MeV per nucleon ions in $^3$He-rich solar particle events. *Astrophysical Journal* 339: 529–544.

Mewaldt, R.A., Mason, G.M., Gloeckler, G., Christian, E.R., Cohen, C.S., Cummings, A.C., Davis, A.J., Dwyer, J.R., Gold, R.E., Krimigis, S.M., Leske, R.A., Mazur, J.E., Stone, E.C., von Rosenvinge, T.T., Wiedenbeck, M.E., and Zurbuchen, T.H. 2001. Long-term fluences of energetic particles in the heliosphere, in Wimmer-Schweingruber, R.F. (ed.), *AIP Conference Proceedings Vol. 598: Solar and Galactic Composition*, pp.165. New York: AIP Press.

Miller, J.A. 1998. Particle acceleration in impulsive solar flares. *Space Science Reviews* 86: 79–105.

Möbius, E., Popecki, M., Klecker, B., Kistler, L.M., Bogdanov, A., Galvin, A.B., Heirtzler, D., Hovestadt, D., Lund, E.J., Morris, D., and Schmidt, W.K. 1999. Energy dependence of the ionic charge state distribution during the November 1997 solar energetic particle event. *Geophysical Research Letters* 26: 145–148.

National Research Council 2004. *Plasma Physics of the Local Cosmos.* Washington DC: The National Academic Press.

Ng, C.K., Reames, D.V., and Tylka, A.J. 1999, Effect of proton-amplified waves on the evolution of solar energetic particle composition in gradual events. *Geophysical Research Letters* 26: 2145–2148.

Palmer, I.D. 1982. Transport coefficient of low-energy cosmic rays in interplanetary space. *Reviews of Geophysics and Space Physics* 20: 335–351.

Parker, E.N. 1958a. Origin and dynamics of cosmic rays. *Physical Review* 109: 1328–1344.

Parker, E.N. 1958b. Dynamics of the interplanetary magnetic field. *Astrophysical Journal* 128: 664–676.

Parker, E.N. 1963. *Interplanetary Dynamical Processes.* New York: Interscience/Wiley.

Parker, E.N. 1965. The passage of energetic charged particles through interplanetary space. *Planetary and Space Science* 13: 9-45.

Parks, G.K. 1991. *Physics of Space Plasmas.* Redwood CA: Addison-Wesley.

Press, W. H., Flannery, B. P., Teukolsky, S. A., and Vetterling, W. T. 1988. *Numerical Recipes in C.* 1st ed. New York: Cambridge University Press.

Press, W. H., Flannery, B. P., Teukolsky, S. A., and Vetterling, W. T. 1992. *Numerical Recipes in C.* 2nd ed. New York: Cambridge University Press.

Protheroe, R.J. 1996. Origin and propagation of the highest energy cosmic rays, in Shapiro M.M. and Wefel, J.P. (ed.), *Proceedings of Towards the Millennium in Astrophysics: Problems and Prospects*, pp.3–25. Singapore: World Scientific.

Rao, U.R., McCracken, K.G. and Bukata, R.P. 1967. The acceleration of energetic particle fluxes in shock fronts in interplanetary space. *Journal of Geophysical Research* 72: 4325.

Reames, D.V. 1990. Acceleration of energetic particles by shock waves from large solar flares. *Astrophysical Journal* 358: L63–L67.

Reames, D.V. 1990. Energetic particles from impulsive solar flares. *Astrophysical Journal Supplement Series* 71: 235–251.

Reames, D.V. 1995. Solar energetic particles: A paradigm shift, in *U.S. National Report to International Union of Geodesy and Geophysics 1991-1994*, pp.585. Washington DC: American Geophysics Union.

Reames, D.V. 1999. Particle acceleration at the Sun and in the heliosphere. *Space Science Reviews* 90: 413–491.

Reames, D.V. 2000. Particles Acceleration by CME-driven shock waves. in Dingus, B.L., Kieda, D.B. and Salamon, M.H. (ed.), *AIP Conference Proceedings Vol. 516: 26th International Cosmic Ray Conference*, pp.289–300. New York: AIP Press.

Reames, D.V., Barbier, L.M., von Rosenvinge, T.T., Mason, G.M., Mazur, J.E., and Dwyer, J.R. 1997. Energy spectra of ions accelerated in impulsive and gradual solar events. *Astrophysical Journal* 483: 515.

Reames, D.V., and Tylka, A.J. 2002. Energetic particle abundances as probes of an interplanetary shock wave. *Astrophysical Journal* 575: L37–L39.

Ruffolo, D. 1997. Charge states of solar cosmic rays and constraints on acceleration times and coronal transport. *Astrophysical Journal* 481: L119–L122.

Ruffolo, D. 1999. Transport and acceleration of energetic charged particle near an oblique shock. *Astrophysical Journal* 515: 787–800.

Ruffolo, D. 2002. Classification of solar energetic particles. *Advances in Space Research* 30(1), 45–54.

Ruffolo, D., and Channok, C. 2003. Finite time shock acceleration. *Proceedings of the 28th International Cosmic Ray Conference* 6: 3681–3684. Tokyo Japan: Universal Academy Press.

Schlickeiser, R. 2002. *Cosmic Ray Astrophysics.* Heidelberg: Springer-Verlag.

Scholer, M., and Ipavich, F.M. 1983. Interaction of energetic storm particles with the earth's bow shock. *Journal of Geophysical Research* 88: 5715–5726.

Scholer, M., and Morfill, G. 1975. Simulation of solar flare particle interaction with interplanetary shock wave. *Solar Physics* 45: 227–240.

Simpson, J.A. 1948. The latitude dependence of neutron densities in the atmosphere as a function of altitude. *Physical Review* 73: 1389–1391.

Smith, C.W., L'Heureux, J., Ness, N.F., Acuna, M.H., Burlaga, L.F., and Scheifele, J. 1998. The ACE magnetic field experiment. *Space Science Reviews* 86: 613–632.

Sollitt, L. 2004. *Ionic Charge State of Solar Energetic Particles.* Ph.D. Thesis. Department of Physics, California Institute of Technology.

Stone, E.C., Frandsen, A.M., Mewaldt, R.A., Christian, E.R., Margolies, D., Ormes, J.F., and Snow, F. 1998. The Advanced Composition Explorer. *Space Science Reviews* 86: 1–22.

Terasawa, T. 1979. Energy spectrum and pitch angle distribution of particles reflected by MHD shock waves of fast mode. *Planetary Space Science* 27: 193–201.

Terasawa, T. 1995. Ion acceleration. *Advances in Space Research* 15(8/9): 53–62.

Torsti, J., Korcharov, L., Laivola, J., Lehtinen, N., Kailer, M.L., and Reiner, M.J. 2002. Solar particle event with exceptionally high $^3$He enhancement in the energy range up to 50 MeV nucleon$^{-1}$. *Astrophysical Journal* 573: L59–L63.

Tylka, A.J. 2001. New insights on solar energetic particles from Wind and ACE. *Journal of Geophysical Research* 106: 25333–25352.

Tylka, A.J., Boberg, P.R., Cohen, C.M., Dietrich, W.F., Maclennan, C.G., Mason, G.M., Ng, C.K., and Reames, D.V. 2002. Flare and shock-accelerated energetic particles in the solar events of 2001 April 14 and 15. *Astrophysical Journal* 581: L119–L123.

Tylka, A.J., Boberg, P.R., McGuire, R.E., Ng, C.K. and Reames, D.V. 2000. Temporal evolution in the spectra of gradual solar energetic particle events, in Mewaldt, R.A., Jokipii, J.R., Lee, M.A., Möbius, E., and Zurbuchen, T.H. (ed.), *AIP Conference Proceedings Vol. 528: Acceleration and Transport of Energetic Particles Observed in the Heliosphere*, pp.147–152. Melville, NY: AIP Press.

Tylka, A.J., Cohen, C.M, Dietrich, W.F., Maclennan, C.G, McGuire, R.E., Reames, D.V., and Ng, C.K. 2001. Energy spectra of very large gradual solar particle events. *Proceedings of the 27th International Cosmic Ray Conference* 3189–3192. Hamburg: Copernicus Gesellschft.

Tylka, A.J., Reames, D.V., and Ng, C.K. 1997. Probability distributions of high energy solar-heavy-ion fluxes from IMP8: 1973–1996. *IEEE Transactions on Nuclear Science* 44: 2140–2149.

Tylka, A.J., Reames, D.V., and Ng, C.K. 1999. Observations of systematic temporal evolution in elemental composition during gradual solar energetic particle events. *Geophysical Research Letters* 26: 2141–2144.

Usoskin, I., Kovaltsov, G., Kananen, H., and Tanskanen, P. 1997. The world neutron monitor network as a tool for the study of solar neutrons. *Annales Geophysicae* 15: 375–386.

Usoskin, I., and Mursula, K. 2001. *Heliospheric Physics and Cosmic Rays.* Oulo, Finland: University of Oulo.

Vainio, R., and Khan, J.I. 2004. Solar energetic particle acceleration in refracting coronal shock waves. *Astrophysical Journal* 600: 451–457.

Van Allen, J.A. and Ness, N.F. 1967. Observed particle effects of an interplanetary shock wave on July 8, 1966. *Journal of Geophysical Research* 72: 935–942.

van Nes, P., Roelof, E.C., Reinhard, R., Sanderson, T.R., and Wenzel, K.P. 1985. Major shock-associated energetic storm particle event wherein the shock plays a minor role. *Journal of Geophysical Research* 90: 3981–3994.

Zank, G.P., Rice, W.M., and Wu, C.C. 2000. Particle acceleration and coronal mass ejection driven shocks: A theoretical model. *Journal of Geophysical Research* 105: 25079–25095.

Zhang, M., and Low, B.C. 2005. The hydromagnetic nature of solar coronal mass ejections. *Annual Review of Astronomy and Astrophysics* 43, (in press). doi:10.1146/annurev.astro.43.072103.150602

# APPENDICES

# Appendix A

## List of Acronyms

| | |
|---|---|
| ACE | Advanced Composition Explorer (spacecraft) |
| AU | Astronomical Unit |
| CME | Coronal Mass Ejection |
| CR | Cosmic Rays |
| DSA | Diffusive Shock Acceleration |
| ESP | Energetic Storm Particle |
| eV | electron Volt (unit of energy) |
| FTSA | Finite Time Shock Acceleration |
| GCR | Galactic Cosmic Ray |
| IP | Interplanetary |
| IPS | Interplanetary Shock |
| MHD | Magnetohydrodynamics |
| SEP | Solar Energetic Particle |
| SMM | Solar Maximum Mission (spacecraft) |
| SNR | Supernova Remnant |
| SOHO | Solar and Heliospheric Observatory (spacecraft) |
| ULEIS | Ultra Low Energy Isotropic Spectrometer (on ACE) |
| UT | Universal Time |

# Appendix B

## Physical Constants[1]

| | |
|---|---|
| velocity of light | 299792458 m/s |
| unified atomic mass unit | $1.660540 \times 10^{-27}$ kg |
| proton mass | $1.672623 \times 10^{-27}$ kg |
| proton rest mass energy | 938.27231 MeV |
| electric charge magnitude | $1.60217733 \times 10^{-19}$ C |
| astronomical unit (AU) | 149597870660 m |



[1] from Caso et al. (1998); Groom et al. (2000)

# Appendix C

## Ultra Low Energy Isotope Spectrometer (ULEIS)

The Ultra Low Energy Isotope Spectrometer (ULEIS) is an instrument on the *ACE* spacecraft. It is an ultra high resolution mass spectrometer designed to measure the particle composition and energy spectra of elements He–Ni with energies from $\sim 45$ keV/nucleon to a few MeV/nucleon (Mason et al. 1998). ULEIS is new instrument for solar space science research in recent times, which investigates particles accelerated in solar energetic particle events and interplanetary (IP) shocks. By determining energy spectra, mass composition, and their temporal variations in conjunction with other ACE instruments, ULEIS has greatly improved our knowledge of solar abundances, as well as other reservoirs such as the local interstellar medium. ULEIS is designed to combine the high sensitivity required to measure low particle fluxes, along with the capability to operate in largest solar particle or IP shock events. In addition to detailed information for individual ions, ULEIS features a wide range of count rates for different ions and energies that allows accurate determination of particle fluxes and anisotropies over short time scales (about a few minutes). The energy range covered by ULEIS measurements includes solar energetic particles, particles accelerated by IP shocks, and low-energy anomalous cosmic rays.

The *ACE* spacecraft is about $1.5 \times 10^6$ km (0.01 AU) in front of Earth, in an excellent position to measure the properties of the solar wind, IP magnetic field, solar energetic particles from the Sun before it impacts the Earth's magnetosphere (Stone et al. 1998). Therefore the ULEIS instrument on the *ACE* spacecraft observes near 1 AU (near the Earth) and provides information about energetic storm particle (ESP) events and IP shock-accelerated particles (Desai et al. 2001; 2003; 2004).

# Appendix D

## ULEIS Observations of Ions at Interplanetary Shocks*

### Interplanetary shock data of June 26, 1999 event

**[June 25, 08:44 UT – June 27, 12:57 UT]**

Carbon

| **Kinetic energy** (MeV nucleon$^{-1}$) | **Intensity** (particles/cm$^2$ s sr MeV nucleon$^{-1}$) |
|---|---|
| 0.1131 – 0.1600 | – |
| 0.1600 – 0.2263 | 2.23 |
| 0.2263 – 0.3200 | 1.53 |
| 0.3200 – 0.4525 | 0.917 |
| 0.4525 – 0.6400 | 0.455 |
| 0.6400 – 0.9051 | 0.214 |
| 0.9051 – 1.2800 | 0.0912 |
| 1.2800 – 1.8102 | 0.0309 |
| 1.8102 – 2.5600 | 0.00854 |
| 2.5600 – 3.6204 | 0.00177 |
| 3.6204 – 5.1200 | 0.000378 |

Oxygen

| **Kinetic energy** (MeV nucleon$^{-1}$) | **Intensity** (particles/cm$^2$ s sr MeV nucleon$^{-1}$) |
|---|---|
| 0.1131 – 0.1600 | 9.64 |
| 0.1600 – 0.2263 | 6.27 |
| 0.2263 – 0.3200 | 3.99 |
| 0.3200 – 0.4525 | 2.33 |
| 0.4525 – 0.6400 | 1.14 |
| 0.6400 – 0.9051 | 0.519 |
| 0.9051 – 1.2800 | 0.221 |
| 1.2800 – 1.8102 | 0.0686 |
| 1.8102 – 2.5600 | 0.0171 |
| 2.5600 – 3.6204 | 0.00439 |
| 3.6204 – 5.1200 | 0.000882 |

* These data were kindly provided by Dr. Mihir Desai.

## Iron

| **Kinetic energy** (MeV nucleon$^{-1}$) | **Intensity** (particles/cm$^2$ s sr MeV nucleon$^{-1}$) |
|---|---|
| 0.1131 – 0.1600 | 1.87 |
| 0.1600 – 0.2263 | 1.04 |
| 0.2263 – 0.3200 | 0.532 |
| 0.3200 – 0.4525 | 0.243 |
| 0.4525 – 0.6400 | 0.104 |
| 0.6400 – 0.9051 | 0.0405 |
| 0.9051 – 1.2800 | 0.0128 |
| 1.2800 – 1.8102 | 0.00249 |
| 1.8102 – 2.5600 | 0.000520 |
| 2.5600 – 3.6204 | – |
| 3.6204 – 5.1200 | – |

## Interplanetary shock data of September 22, 2000 event
**[September 22, 06:39 UT – September 23, 04:31 UT]**

### Carbon

| **Kinetic energy** (MeV nucleon$^{-1}$) | **Intensity** (particles/cm$^2$ s sr MeV nucleon$^{-1}$) |
|---|---|
| 0.1131 – 0.1600 | – |
| 0.1600 – 0.2263 | 1.21 |
| 0.2263 – 0.3200 | 0.510 |
| 0.3200 – 0.4525 | 0.169 |
| 0.4525 – 0.6400 | 0.0506 |
| 0.6400 – 0.9051 | 0.0179 |
| 0.9051 – 1.2800 | 0.00351 |
| 1.2800 – 1.8102 | – |
| 1.8102 – 2.5600 | – |
| 2.5600 – 3.6204 | – |
| 3.6204 – 5.1200 | – |

### Oxygen

| **Kinetic energy** (MeV nucleon$^{-1}$) | **Intensity** (particles/cm$^2$ s sr MeV nucleon$^{-1}$) |
|---|---|
| 0.1131 – 0.1600 | 7.71 |
| 0.1600 – 0.2263 | 3.32 |
| 0.2263 – 0.3200 | 1.28 |
| 0.3200 – 0.4525 | 0.447 |
| 0.4525 – 0.6400 | 0.123 |
| 0.6400 – 0.9051 | 0.0309 |
| 0.9051 – 1.2800 | 0.00949 |
| 1.2800 – 1.8102 | – |
| 1.8102 – 2.5600 | – |
| 2.5600 – 3.6204 | – |
| 3.6204 – 5.1200 | – |

Iron

| **Kinetic energy** (MeV nucleon$^{-1}$) | **Intensity** (particles/cm$^2$ s sr MeV nucleon$^{-1}$) |
|---|---|
| 0.1131 – 0.1600 | 0.479 |
| 0.1600 – 0.2263 | 0.190 |
| 0.2263 – 0.3200 | 0.0695 |
| 0.3200 – 0.4525 | 0.0318 |
| 0.4525 – 0.6400 | 0.00717 |
| 0.6400 – 0.9051 | 0.00177 |
| 0.9051 – 1.2800 | – |
| 1.2800 – 1.8102 | – |
| 1.8102 – 2.5600 | – |
| 2.5600 – 3.6204 | – |
| 3.6204 – 5.1200 | – |

## Interplanetary shock data of October 5, 2000 event
### [October 4, 22:55 UT – October 5, 08:55 UT]

### Carbon

| **Kinetic energy** (MeV nucleon$^{-1}$) | **Intensity** (particles/cm$^2$ s sr MeV nucleon$^{-1}$) |
|---|---|
| 0.1131 – 0.1600 | – |
| 0.1600 – 0.2263 | 0.188 |
| 0.2263 – 0.3200 | 0.0562 |
| 0.3200 – 0.4525 | 0.0140 |
| 0.4525 – 0.6400 | 0.00504 |
| 0.6400 – 0.9051 | – |
| 0.9051 – 1.2800 | – |
| 1.2800 – 1.8102 | – |
| 1.8102 – 2.5600 | – |
| 2.5600 – 3.6204 | – |
| 3.6204 – 5.1200 | – |

### Oxygen

| **Kinetic energy** (MeV nucleon$^{-1}$) | **Intensity** (particles/cm$^2$ s sr MeV nucleon$^{-1}$) |
|---|---|
| 0.1131 – 0.1600 | 1.36 |
| 0.1600 – 0.2263 | 0.492 |
| 0.2263 – 0.3200 | 0.150 |
| 0.3200 – 0.4525 | 0.0486 |
| 0.4525 – 0.6400 | 0.0151 |
| 0.6400 – 0.9051 | 0.00446 |
| 0.9051 – 1.2800 | 0.00181 |
| 1.2800 – 1.8102 | – |
| 1.8102 – 2.5600 | – |
| 2.5600 – 3.6204 | – |
| 3.6204 – 5.1200 | – |

Iron

| **Kinetic energy** (MeV nucleon$^{-1}$) | **Intensity** (particles/cm$^2$ s sr MeV nucleon$^{-1}$) |
|---|---|
| 0.1131 – 0.1600 | 0.196 |
| 0.1600 – 0.2263 | 0.0821 |
| 0.2263 – 0.3200 | 0.0370 |
| 0.3200 – 0.4525 | 0.0195 |
| 0.4525 – 0.6400 | 0.00629 |
| 0.6400 – 0.9051 | 0.00295 |
| 0.9051 – 1.2800 | – |
| 1.2800 – 1.8102 | – |
| 1.8102 – 2.5600 | – |
| 2.5600 – 3.6204 | – |
| 3.6204 – 5.1200 | – |

# Vitae

Name: Mr. Chanruangrit Channok

Born: July 17th, 1974 in Nakornrajasima, Thailand.

Address: Dept. of Physics, Ubonrajathanee Univ., Ubonrajathanee, Thailand.

E-mail: physics007@yahoo.com

URL: http://www.geocities.com/physics007

Education:

1996 B.Sc. degree in physics, Khon Kaen Univ., Khon Kean, Thailand.
2000 M.Sc. degree in physics, Chulalongkorn Univ., Bangkok, Thailand.

Position: Faculty member at the Dept. of Physics, Ubonrajathanee Univ.